AN EXPERIMENTAL STUDY
OF
HEAVY MINERAL SEGREGATION
UNDER ALLUVIAL-FLOW CONDITIONS

By
Lawrence L. Brady and Harvey E. Jobson

U18401 0576299

CONTENTS

―――――

ILLUSTRATIONS

Page

iv

TABLES

_____

AN EXPERIMENTAL STUDY OF HEAVY MINERAL
SEGREGATION UNDER ALLUVIAL-FLOW CONDITIONS

By Lawrence L. Brady and Harvey E. Jobson

ABSTRACT

Segregation of opaque minerals (mainly ilmenite and magnetite) from the light minerals in a natural sand was observed in a large (61 × 2.44 × 1.22 meters) recirculating water-sediment flume. Bed material (median size 0.286 millimeter) used in the study was taken from the Rio Grande near Bernardo, New Mexico. Opaque heavy minerals (median size 0.144 millimeter) present in the bed material comprised 0.38 percent of the bed material volume. Significant hydraulic variables, and sorting and bedding patterns of the bed material, were observed for four different bed configurations: a flat bed (upper flow regime), a transition bed, and two different dune beds (lower flow regime).

Accumulations of opaque heavy minerals were formed as three basic types:

1. thin accumulations of opaque heavy minerals covering small areas that were associated with the upstream or stoss slopes of dunes;

2. accumulations associated with the topset deposits of large dunes and with dunes formed in the transition flow;

3. accumulations associated with the flat-bed condition.

The most important factors influencing the type and amount of accumulation of opaque heavy minerals are bed configuration and grain density. Segregation of heavy minerals associated with flat beds occurred mainly at the base of the planar beds, where the most widespread deposit of opaque heavy minerals of the three segregating processes form. The thickest deposits of opaque heavy mineral grains were associated with topset deposits of dune beds, but local conditions must be optimum for thick accumulations to occur. Mineral density is important to segregation because the difference in shear stress necessary to move the light minerals and to move opaque heavy minerals is large. This is shown by means of theoretical considerations of the forces necessary to move grains of two different densities and by means of analysis of the bed material and core samples using a Shields' type criteria for initiation of motion.

Sediment size, sorting, and shape were determined for each mineral group from core samples taken from the bed. The sorting of the opaque heavy minerals for the flat bed run was significantly different than that for the other runs.

Median sizes of the light minerals which were obtained from laminae adjacent to or within the heavy mineral laminae also showed a significant variation among runs. Fall velocities of the grains of the two different mineral groups were found to have little importance in local segregating mechanisms.

INTRODUCTION

In an alluvial channel, bedding patterns produced in sediment
are responses to the hydraulic variables of a specific flow.
Variations in sorting and rates of sorting, or the segregation of the
transported materials according to size, shape, and density, are
important elements in the production of bedding structures and in
recognition of the structures in sediments and sedimentary rocks.

Relatively little is understood about the local hydraulic condi-
tions or the sediment responses to these conditions that are responsible
for sorting of sediments. The relative densities of particles, and
stream flow characteristics, have long been assumed to be important
factors in sorting but their relative contributions to the sorting
process have not been well understood.

The relationship of heavy minerals to the more common low-density
minerals was first described in relation to given hydraulic conditions
by Rubey (1933). Equal fall velocities of minerals of different densities
were considered by Rubey to be the most important factor accounting for
the close association of small high-density grains with low-density but
larger mineral grains in a sediment. Other factors considered important
by Rubey (1933, p. 3) were density and hardness of the minerals,
differences in original sizes of the grains in the source rock, amount
of abrasion during transport, and degree of sorting at the site of
deposition.

Rittenhouse (1943) used the concept of hydraulic equivalence to explain mineral relations in sands of the Rio Grande in New Mexico. He described hydraulic equivalence (p. 1749) as: ". . . whatever the hydraulic conditions may be that permit the deposition of a grain of particular physical properties, these conditions will also permit deposition of other grains of equivalent value." The distribution of heavy minerals in the stream bed was considered by Rittenhouse (1943, p. 1742-1743) to be caused by varying hydraulic conditions at the time and place of deposition, equivalent hydraulic size of each of the heavy minerals, availability of the minerals, and unknown factors.

Studies on sorting of minerals with different densities were conducted simultaneously with studies of turbulence, bed resistance and sediment transport at the Engineering Research Center at Colorado State University. Experiments were conducted in a large recirculating sediment flume using natural sand from the Rio Grande south of Albuquerque, New Mexico. This research was undertaken in an effort to find what sediment properties and hydraulic variables are responsible for the rapid segregation of certain heavy minerals during movement and deposition of a sediment load.

Four flow conditions were studied at near equilibrium conditions. Observations were made of the significant hydraulic variables, sediment transport rate, sediment segregation, and the physical characteristics of the sediments entrained by each flow to obtain information necessary to explain the sorting processes.

This study contributes to the understanding of local segregation processes that affect grains of different densities. Techniques used and results obtained can be applied to other studies of bedding in modern sediment and in interpretation of ancient deposits. Further, observations made in these flume studies of modes of segregation, transport, and accumulation of heavy minerals should help in future research on and exploration for economically valuable placer deposits.

This program was completed under a cooperative arrangement between the U. S. Geological Survey, the University of Kansas and Colorado State University. The data contained herein are essentially the same as those contained in a dissertation by Brady (1971). The data were collected under the general supervision of the second author.

Special thanks are due the dissertation committee members, W. M. Merrill, E. C. Pogge, M. E. Bickford, A. J. Powell, and J. D. Winslow of the University of Kansas for advice and counsel during the research.

THEORETICAL CONSIDERATIONS

Relative Velocities of Water-Transported Particles
with Differing Densities

Consideration of the forces acting on discrete particles in a few idealized situations can provide the basis for estimates of conditions in the natural environment. Actual values for the velocities and forces involved in the grain movement would be very difficult to determine experimentally. By making certain assumptions deduced for grains with different densities, however, approximations of the relative velocities of grains can be developed.

For immersed particles moving along a bed, five principal forces are important in determining the movement of the particle. These forces include the (1) gravity forces related to the immersed weight of the particle, the (2) drag and (3) lift forces that result from pressure and frictional effects of the fluid on the particle, (4) frictional forces that result from contact between the grain and bed, and (5) forces resulting from adjacent moving grains.

By considering an individual sphere that moves without interference from adjacent moving grains, the principal forces can be defined. The gravity force, F_G, is the resultant force acting on the particle that is dependent on the immersed weight of the particle and the gravitational constant, g. The gravity force is defined as

$$F_G = \frac{\pi d^3}{6} (\rho_s - \rho) g \qquad (1)$$

where d = diameter of the particle, ρ_s = mass density of the particle, and ρ = mass density of the fluid. (All symbols used in the text are listed in Appendix A.)

The hydrodynamic forces acting on a body are discussed in any standard fluid mechanics text e.g. Daily and Harleman (1966, p. 376-394). The hydrodynamic drag force F_D, that acts on a particle is dependent on the frictional drag resulting from surface shear between the grain and the fluid and on the form resistance that is related to shape of the grain and results from pressure drag on the particle. It is customary to define a total drag coefficient, C_D, to include both frictional and form drag. Some researchers have directly measured the drag and lift forces acting on regular shaped objects such as spheres (Watters and Rao, 1971, p. 421-439; Coleman, 1967, p. 185-192; and Ippen and Verma, 1955, p. 921-939) and hemispheres (El-Sammi, 1949) in laboratory flumes.

The drag force is defined as

$$F_D = C_D \, A_s \, \rho \, \frac{V_o^2}{2} = C_D \, \frac{\pi d^2}{8} \, \rho \, (V_f - V_s)^2 \tag{2}$$

where A_s = projected area of the sphere, V_o = relative velocity of the flow past the sphere, V_f = velocity of the flow at some representative distance above the bed, and V_s = velocity of translation of the particle.

Lift forces on the body are due to a difference in pressure between the upper and lower sides of the particle. The increased velocity resulting from fluid acceleration around the upper side of a particle causes a local reduction in pressure, while the pressure on the lower side of the grain surface at or near the bed approaches the static pressure of the fluid. The lift force, F_L , is defined as

$$F_L = C_L A_s \rho \frac{V_o^2}{2} = C_L \frac{\pi d^2}{8} \rho (V_f - V_s)^2 \qquad (3)$$

where C_L = coefficient of lift.

The frictional force acting on a moving particle is difficult to determine. The frictional force is discussed in most basic physics or mechanics texts such as Sears and Zemansky (1963, p. 35). Ippen and Verma (1955, p. 921-937) has also discussed the frictional force. Bagnold (1966, p. 5) states that the friction coefficient for grains is of the same order as the static coefficient, not only when the grains are at rest but also when they are in motion. For the purposes of this study, the frictional force was assumed to be equal to the coefficient of kinetic friction, C_F, times the normal force between the particle and the bed, F_N. The frictional force, F_F, is defined as

$$F_F = C_F F_N = C_F (F_G \cos\theta - F_L) \qquad (4)$$

where θ = angle between the bed surface and horizontal. A positive value of θ indicates that the bed surface is rising in a downstream direction, such as on the stoss slope of a ripple or dune.

10

Although the coefficient of kinetic friction for sediment particles is very difficult to determine one would suspect that it is closely related to the coefficient of static resistance, C_R, of a particular particle resting on a given bed configuration. Restricting ones attention to a rigid spherical particle of diameter d_m resting on a bed of rigid spherical particles of diameter d_B arranged in a prescribed manner, it is a simple matter to determine the coefficient resistance, C_R.

For example, if the bed spheres are arranged in a close packed rectangular manner and are resting on a horizontal plane, it can be easily shown that the centrally applied horizontal force required to move a sphere of diameter d_m in the direction of least resistance is $C_R F_N$, where C_R is given by the relation

$$C_R = \frac{1}{\sqrt{k^2 + 2k - 1}} \tag{5}$$

and k is defined as the ratio of d_m to d_B. Likewise, if the bed spheres are arranged in a rhombic pattern the value of C_R corresponding to movement in the direction of least resistance is given by

$$C_R = \frac{1}{2\sqrt{k^2 + 2k - 1/3}} \tag{6}$$

It is seen that the resistance of a particle to motion is a function of both the size of the moving particle and the size of the bed particles.

In order to determine the effect of particle size on the resistance to motion, the resistance ratio is defined as the ratio of C_R at any value of k to the value of C_R with k=1. The relation of the value of the resistance ratio to k is shown in figure 1. The curves approach infinity at a value of k for which a small moving particle

---

Figure 1 (caption on next page) belongs near here

---

could fall between the interstices of the larger bed particles. The figure illustrates that the resistance to motion of a small particle resting on a bed of large particles can be quite large. It is not presumed that the values given in figure 1 can be applied directly to field situations, however it is suggested that the qualitative trend is correct.

The four forces as they are applied to a spherical particle are shown schematically in figure 2. The gravitational force can either

---

Figure 2 (caption on next page) belongs near here

---

oppose or supplement the drag force depending on the sine of θ.
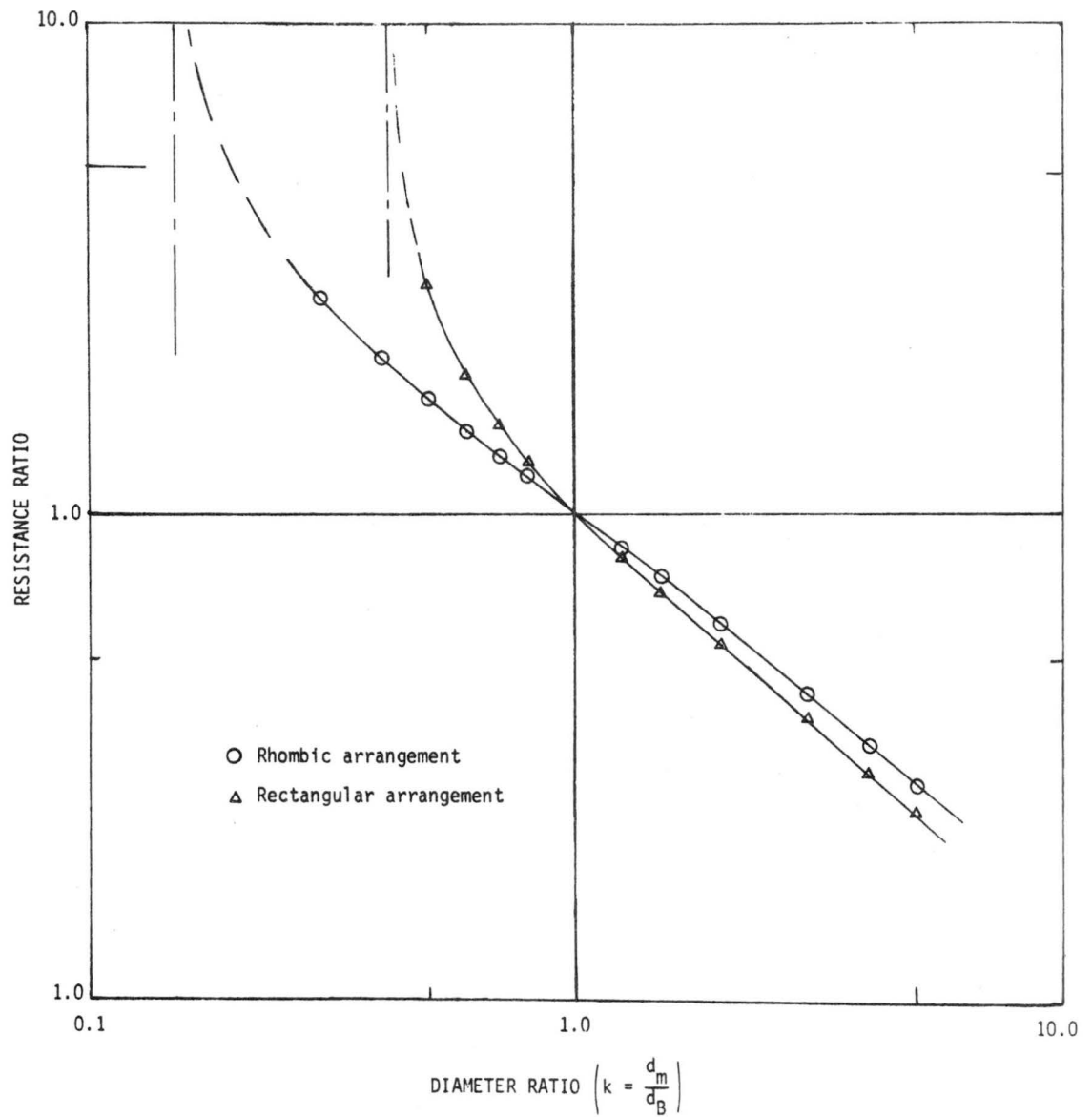
Figure 1. Resistance of a particle to motion as a function of the ratio of its size to the size of the bed material.
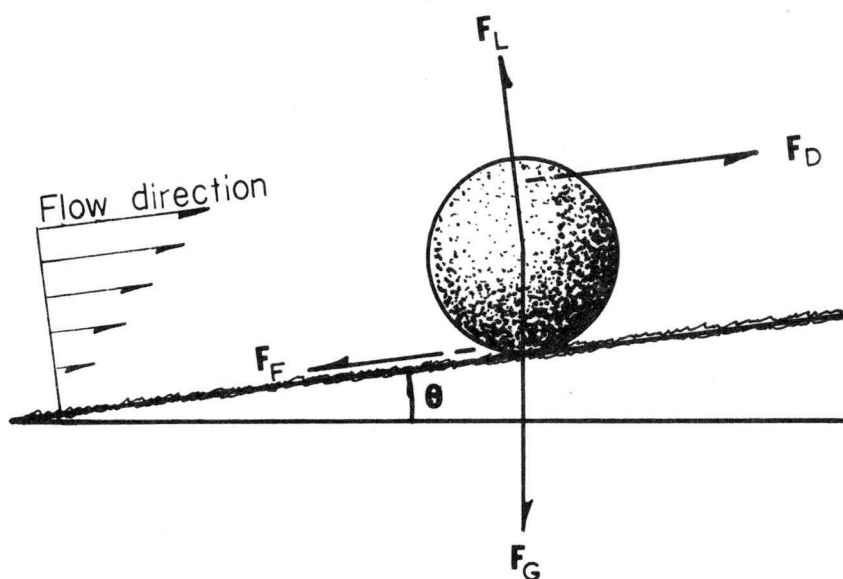
Figure 2. Schematic diagram of forces acting on a
discrete moving particle in a fluid.

By use of the four fundamental equations (1 through 4), a general equation of motion for particles can be derived. Direct comparisons between grains of different densities can then be made by establishing ratios of the translating motion of the grain of greater density to that of the grain of lesser density and reducing the equations to a form that expresses the relative difference in the velocities of the two grain types for the same flow conditions.

For a particle in motion and having a uniform velocity, the general translation motion equation for the particle can be expressed as

$$F_F = F_D - F_G \sin\theta \quad . \tag{7}$$

By dividing the frictional force on one particle by the frictional force on a particle of different density, the following ratio can be established using equations (4) and (7).

$$\frac{F_F}{F_{F_1}} = \frac{F_D - F_G \sin\theta}{F_{D_1} - F_{G_1} \sin\theta} = \frac{C_F(F_G \cos\theta - F_L)}{C_{F_1}(F_{G_1} \cos\theta - F_{L_1})} \quad . \tag{8}$$

The subscript (1) is used to denote the forces and coefficients affecting the sphere of the lower density.

By substituting equations (1), (2), and (3) into equation (8), and simplifying terms, the following equation can be developed.

$$\frac{3\rho C_D (V_f - V_s)^2 - 4dg(\rho_s - \rho)\sin\theta}{3\rho C_{D_1}(V_{f_1} - V_{s_1})^2 - 4d_1 g(\rho_{s_1} - \rho)\sin\theta} =$$

$$\frac{C_F[4dg(\rho_s - \rho)\cos\theta - 3C_L\rho(V_f - V_s)^2]}{C_{F_1}[4d_1 g(\rho_{s_1} - \rho)\cos\theta - 3C_{L_1}\rho(V_{f_1} - V_s)^2]} \tag{9}$$

15

By considering $\theta = 0$ equation (9) can be simplified to

$$\frac{C_D (V_f - V_s)^2}{C_{D_1} (V_{f_1} - V_{s_1})^2} = \frac{C_F [4dg(\rho_s - \rho) - 3C_L \rho (V_f - V_s)^2]}{C_{F_1} [4d_1 g(\rho_{s_1} - \rho) - 3C_{L_1} \rho (V_{f_1} - V_{s_1})^2]} \tag{10}$$

Equation (10) can be used to determine the relative velocities of rolling spheres with different densities.

Assuming the two spheres have equal diameters and therefore equal drag coefficients and equal lift coefficients and assuming equal coefficients of friction, equation (10) reduces to

$$\frac{(V_f - V_s)^2}{(V_f - V_{s_1})^2} = \frac{(\rho_s - \rho)}{(\rho_{s_1} - \rho)} \quad . \tag{11}$$

By applying densities of materials of interest in this study: 5.0 g/cm^3 (gram per cubic centimeter) for ρ_s , 2.65 g/cm^3 for ρ_{s_1}, and 1.0 g/cm^3 for ρ , equation (11) can be expressed in dimensionless form as

$$\frac{V_s}{V_{s_1}} = 1.56 - 0.56 \left[\frac{V_{s_1}}{V_f} \right]^{-1} \tag{12}$$

A graph of equation 12 is shown in figure 3.

Figure 3 (caption on next page) belongs near here

16
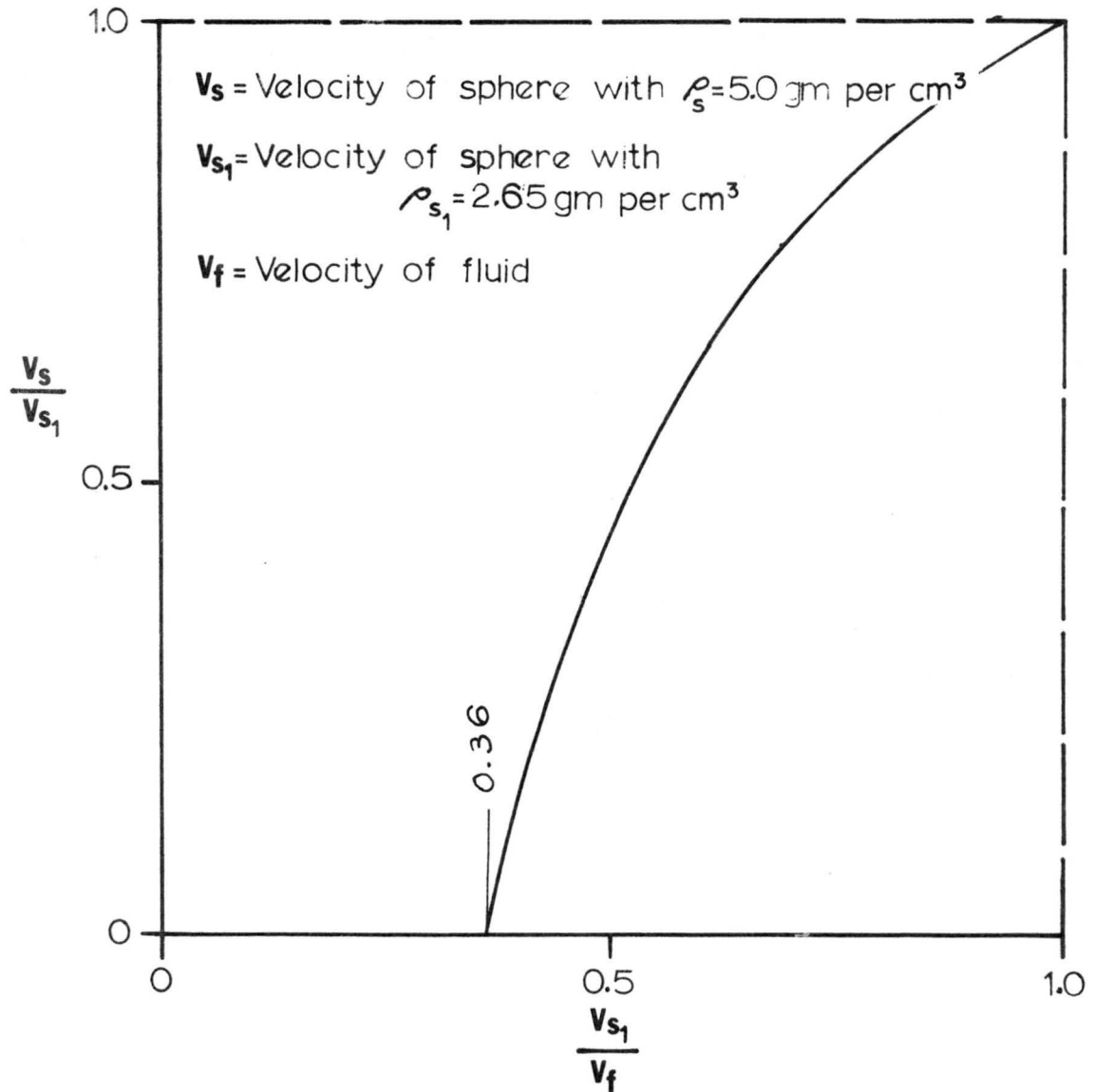
Figure 3.   Velocity ratios for spheres of equal size
but of different densities.

The relative velocities of spheres of the two different densities are clearly shown in figure 3. The velocity of the denser sphere V_s, is always less than that of the lighter sphere, V_{s_1}, unless both are equal to the fluid velocity, V_f, a condition where there is no frictional force. This condition could occur when both particles are suspended. As the velocity of the lighter particle becomes progressively smaller, the relation $\frac{V_s}{V_{s_1}}$ also becomes progressively smaller until a point is reached where movement of the denser sphere ceases. At this point--the point of incipient motion of the denser particle--the velocity of the low-density particle is 0.36 times the fluid velocity.

A second situation that can be approximated is that of two spherical particles of equal submerged weight but having different densities. Substituting values for the densities of the spherical particles of 5.0 g/cm^3 and 2.65 g/cm^3, the ratio of diameters required to obtain equal submerged weights is 1:1.34. Additional conditions, however, must be assumed in order to derive a general velocity formula such as equation (12). These conditions are:

1. For consideration in the drag force equation, a drag coefficient ratio (C_D/C_{D_1}) of 1.2:1 is assumed. Drag coefficients of the two spheres will differ because of their difference in size. The value of 1.2:1 was approximated from the C_D vs. Re diagram in the U. S. Inter-Agency Committee on Water Resources Report 12 (1957, p. 20) by using grain sizes similar to the experimental runs [0.12 mm (millimeter) for the heavy grain and 0.163 mm for the light grains]. Here Re refers to the Reynolds number relative to a particle.

2. The lift forces for this situation are ignored.

3. Two situations will be considered. First the coefficient of static friction is considered to be the same for both spherical particles $(C_{F_1} = C_F)$. Second, the ratios of the two coefficients of friction will be assumed equal to the resistance ratio given in figure 1. It will be assumed that the bed is composed of particles of a size equal to that of the larger particles arranged in a rhombic pattern. From figure 1 the value of C_F/C_{F_1} is found to be 1.25.

4. An assumption is made for this analysis that the increase in fluid velocity with distance from the bed is linear, at least up to a point where the characteristic velocity is determined, as it is in the laminar sublayer. The fluid velocity is assumed to be zero at the bed surface. For the above assumption, the fluid velocity at the point of drag force application of the small sphere would be 0.746 of the value of the fluid velocity at the corresponding point on the larger sphere.

Accepting these assumptions, the basic equation (10) can be reduced to

$$\frac{V_s}{V_{s_1}} = 1.23 - 0.65 \left[\frac{V_{s_1}}{V_f} \right]^{-1} \tag{13}$$

for equal friction coefficients and

$$\frac{V_s}{V_{s_1}} = 1.54 - 1.06 \left[\frac{V_{s_1}}{V_f} \right]^{-1} \tag{14}$$

for a resistance ratio determined from figure 1. Equations 13 and 14 are plotted on figure 4.

Figure 4 (caption on next page) belongs near here
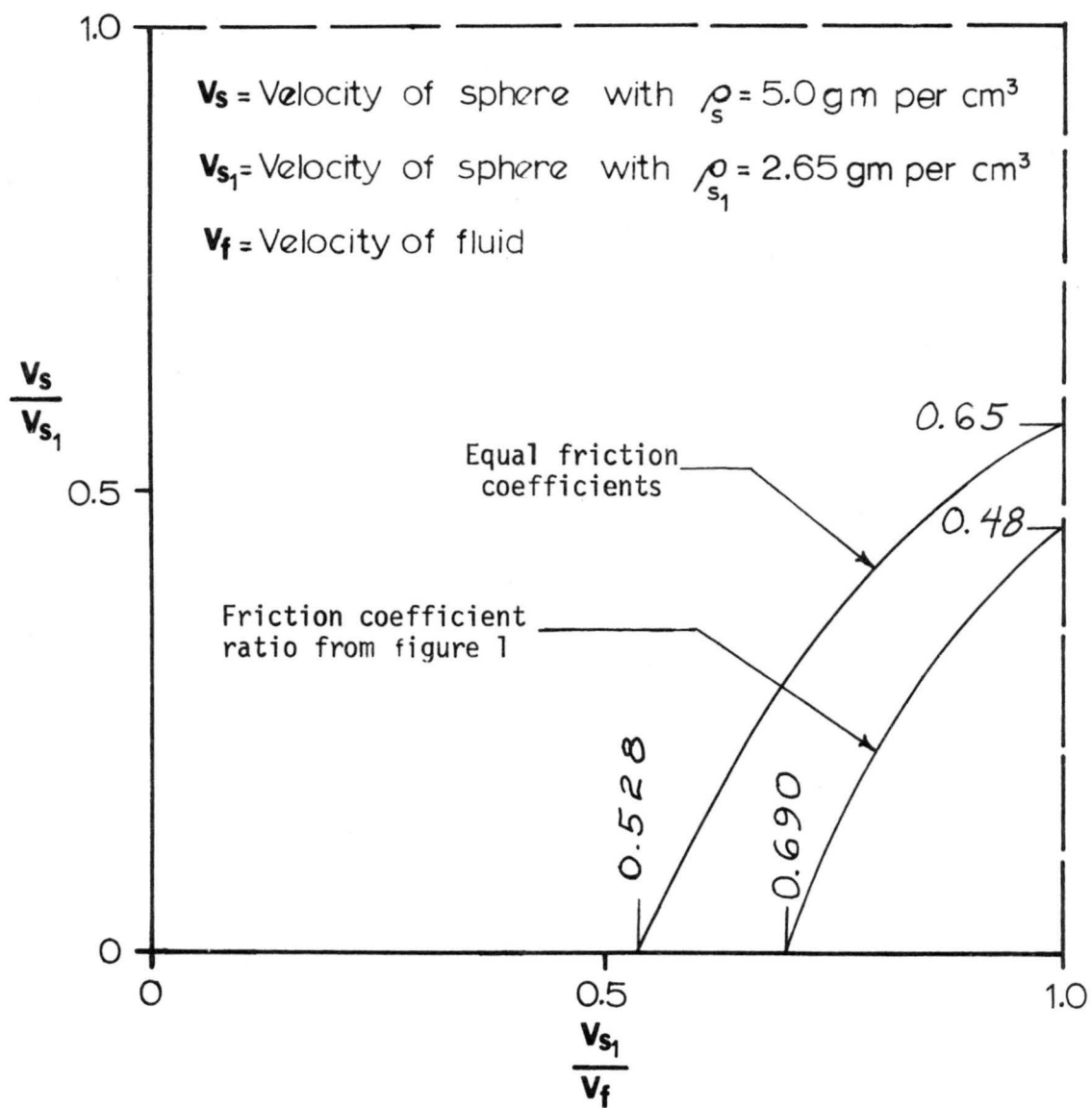
Figure 4. Velocity ratios of spheres with equal submerged weight but of different densities.

For the development of equations 10 through 14, the bed surface was considered horizontal; but the relations shown in figures 3 and 4 should be qualitatively similar for any given bed form slope. The basic difference in forces affecting the grains when a slope factor is introduced is related to the effect of grain weight on the grain movement. A gravity force component parallel to the bed will act against the drag force if the local bed surface is inclined in a direction opposite to the energy slope or the stream gradient. This condition is analogous to grain movement up the stoss side of a dune or ripple (fig. 2). When the local bed surface is inclined in the direction of the energy slope or stream gradient such as occurs on a flat bed or the lee slope of a dune, the particle weight then becomes additive to the drag force in influencing grain movement downstream.

In addition to the effect of gravity, frictional forces resulting from differences in the bed surface will have marked effect on the grain velocity. A coarser sand bed will provide a higher coefficient of friction than a finer sand bed for a given size of grain in movement.

The above analysis assumes that the grains of interest are not so large or heavy that they tend to displace the underlying grains and sink into the bed during the flow. For grains under these conditions, and they occasionally occur in the field, different methods of analysis would be required.

Grains moving at the surface of a sediment bed are continually being deposited and re-entrained at a rate dependent on the local conditions of the flow. When considering grain velocities that are much lower than the fluid velocity, there exists a large difference between the velocities of grains of different densities (fig. 3 and 4). It is at this stage, where large differences in the velocities of of the two types of grains exist or under conditions prior to movement of high-density grains, that segregation of the two grain types is most likely to occur. The low-density grains can be entrained and moved much more readily than the high-density grains and during deposition the high-density grains would be deposited first. This type of situation provides for efficient segregation by causing the selective deposition and accumulation of high-density grains in areas where the flow is not readily capable of transporting all the material supplied to the area. In other words, if a mixture of particles is supplied to an area where the flow is incapable of transporting the total load, the heavy particles will be selectively deposited first.

These considerations establish in a semi-quantitative but simplified manner what has long been observed, that small dense grains are more resistant to surface movement than are larger low-density grains. Graphs similar to figures 3 and 4 can be constructed for natural materials of any density. Then, by considering realistic conditions as observed in sediments in the natural alluvial environment, the graphs can help explain some of the observed bedding features that involve materials of different densities.

Shear Stress as a Density Segregation Parameter

Consideration of critical shear stress (τ_c), which is the stress exerted by the flow on the bed that is just capable of initiating grain movement, adds insight into the segregation of grains of varying densities. Shields (1936) plotted experimental results of the beginning of particle motion based on a dimensionless shear stress (τ_*) and a particle Reynolds number (R_*) where

$$\left. \begin{aligned} \tau_* &= \frac{\tau_c}{(\gamma_s - \gamma)d_s} \\ R_* &= \frac{U_* d_s}{\nu} \end{aligned} \right\} \tag{15}$$

with γ_s equal to the specific weight of the sediment grains, γ the specific weight of the fluid, d_s the grain diameter, U_* is the shear velocity or $\sqrt{\tau_o/\rho}$ with ρ the fluid density, ν is the kinematic viscosity of the fluid, and τ_o is the average shear stress at the bed.

Additional data and refinement of this plot by later workers has resulted in the generally accepted Shields diagram shown in figure 5,

---

Figure 5 (caption on next page) belongs near here

(A.S.C.E. Task Committee on Preparation of Sedimentation Manual, 1966, p. 297). Based on the curve (fig. 5), one can develop the relation of critical shear to grain size for grains of different densities. Grigg and Rathbun (1969) have developed such a series of curves that show on a theoretical basis, that grains of different density but equal fall velocity require different shear stress for initiation of movement. For a grain diameter below 0.1 mm, Grigg and Rathbun (1969, p. 79) show that critical shear is a function only of grain density, but with grains larger than 0.1 mm the critical shear becomes a function of size as well as density.

Conditions under which the Shields diagram was developed were quite different from conditions that exist in an alluvial channel. Data used to develop the Shields curve were obtained from artifically flattened sand surfaces with uniform size grains under fully developed turbulent flows in which shear at the bed was just large enough to initiate a few grain movements. In contrast to conditions at initiation of sediment motion, large amounts of sediment are in transport at relatively high velocities on stream beds when segregation occurs, and the size distribution of the bed material is seldom uniform.
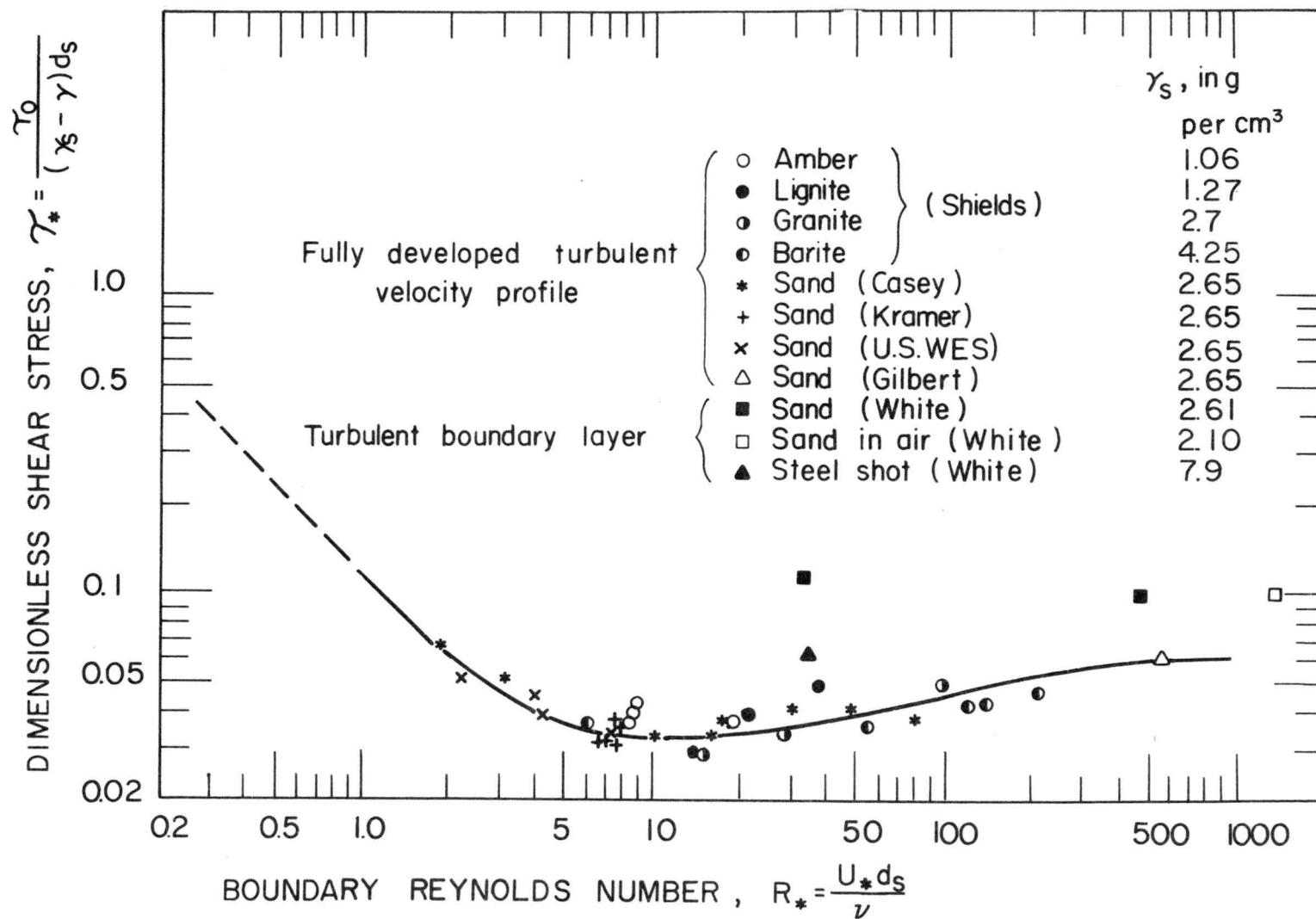
Figure 5. Shields' diagram showing sediment entrainment as a function of the particle Reynolds number (adapted from the A.S.C.E. Task Committee on Preparation of Sedimentation Manual, 1966, p. 297).

Even though Shields' (1936) work was developed for the situation of very small amounts of sediment motion, it gives insight into relations among moving grains. During a given flow, grains are continually being deposited and then re-entrained into the flow, thus, grains at the interface are continually subjected to conditions near incipient motion. One can see, at least qualitatively, from Shields' work that the denser grains will require a much larger shear stress for movement than lighter grains of the same size.

An extension of the threshold of motion considerations is the problem of determining the quantity of sediment in transport along the bed surface. Best known among the bed-load equations is the Einstein bed-load function (Einstein, 1950). Einstein's bed-load equations express a relation between the intensity of shear on a particle (ψ) and intensity of transport (Φ) where

and

$$
\left.
\begin{aligned}
\Phi &= \frac{q_B}{\gamma_s} \left(\frac{\gamma}{\gamma_s - \gamma} \frac{1}{g d_s^3} \right)^{\frac{1}{2}} \\
\psi &= \frac{\gamma_s - \gamma}{\gamma} \frac{d_s}{R'S}
\end{aligned}
\right\}
\tag{16}
$$

where q_B is the rate of transport of the bed-load in weight of total bed load per unit time and width, g is the gravitational constant, d_s is the grain diameter, S is the energy slope and R' is the hydraulic radius with respect to the particles $(R'$ is based on the resistance to flow due to particle resistance as opposed to that due to the bed or stream bank configuration). The shear intensity parameter (ψ) of Einstein is essentially the reciprocal of Shields' dimensionless shear stress (τ_*) and is important in determining the total transport rate of the bed load (q_B). The fact that the transport rate is a function of (ψ) lends credence to the importance of Shields' parameter in situations other than the initiation of motion of uniformly sized grain on flattened beds.

Bed Forms Produced by Flow in an Alluvial Channel

Shortly following initiation of movement of the bed material, bed forms start to develop. These initial forms are described by Kennedy (1963, p. 522) as ". . . the result of scour and deposition due to the perturbation velocities induced by any protuberance on the bed." Flows in alluvial channels are classified into two flow regimes, upper and lower, with a transition zone between. These regimes are based on the bed configuration, mode of sediment transport, process of energy dissipation, and phase relation between the bed and water surfaces (Simons and Richardson, 1963). Relations of bed forms within these two regimes are shown in table 1 and the bed forms are shown in figure 6.

Table 1 (p. 31 of ms.) near here

Figure 6 (caption on next page) belongs near here

Table 1. Classification of flow regimes (adapted from Simons, Richardson, and Nordin, 1965a, p. 36). (ppm, parts per million)

Flow regime	Bed form	Bed Material concentrations (ppm)	Mode of sediment transport	Type of roughness	Phase relation between bed and water surface
Lower regime	Ripples	10 - 200	Discrete steps	Form roughness predominates	Out of phase
	Ripples on dunes	100 - 1,200			
	Dunes	200 - 2,000			
Transition	Washed out dunes	1,000 - 3,000		Variable	
Upper regime	Plane beds	2,000 - 6,000	Continuous	Grain roughness predominates	In phase
	Antidunes	2,000 ------▶			
	Chutes and pools	2,000 ------▶			
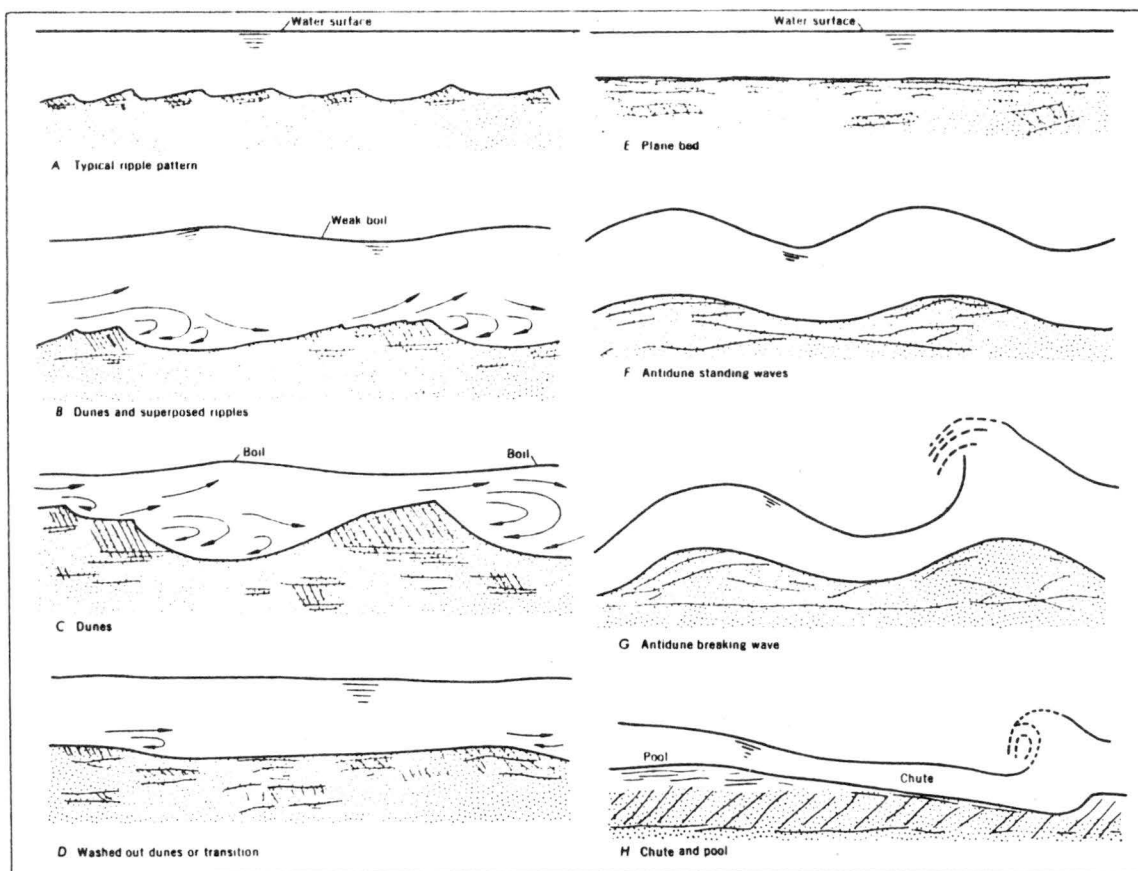
Figure 6.   Idealized diagram of bed forms in an alluvial channel
(from Simons and Richardson, 1966, p. J5).

The A.S.C.E. Task Force on Bed Forms in Alluvial Channels (1966, p. 53) defines ripples as bed forms with wave lengths less than approximately one foot and heights less than 0.1 foot. Dunes are bed forms larger than ripples and out of phase with any water-surface gravity waves that accompany them, while a flat bed is a bed surface devoid of bed form. Antidunes and chutes-and-pools develop within the upper portion of the upper flow regime but were not studied in this series of experiments. These features are described by Simons, Richardson, and Nordin, 1965a, p. 40-42.

Bed forms within the lower flow regime include ripples, ripples superimposed on dunes, and dunes. In the lower regime the water surface waves and undulations are out of phase with the bed undulations. In general, resistance to flow is high while sediment transport is small. In natural streams, dunes or dunes with superimposed ripples are the most common bed forms (Simons and Richardson, 1966, p. 11).

Within the transition flow the bed configuration is very erratic and may include forms common to both the upper and lower regimes. Dunes present in the transition zone will often decrease in amplitude and increase in length before the bed becomes flat (washed-out dunes) (Simons and Richardson, 1966, p. 11).

In the upper flow regime the usual bed forms are flat beds (plane beds) or antidunes, with small resistance to flow and large sediment transport. Water surface waves in this regime are in phase with the bed surface except during the breaking of an antidune (Simons and Richardson, 1966, p. 11).

Bed forms produced by the four different experimental runs in this study were dunes in the lower flow regime, long profile dunes in the transition zone, and a flat bed in the upper flow regime. Terminology used in this report for the different surface features of dunes and the bedding structures associated with the dunes is shown in figure 7.

Figure 7 (caption on next page) belongs near here
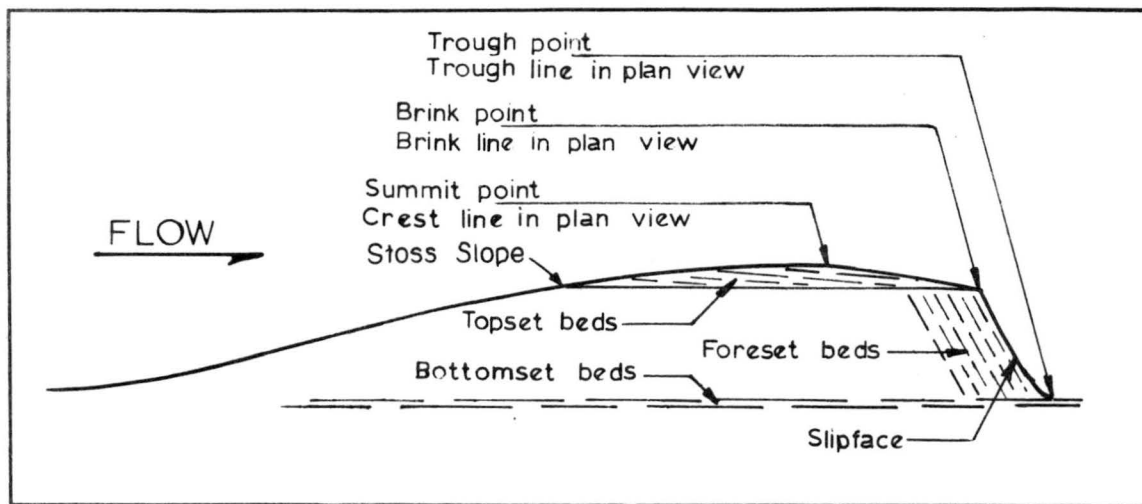
Figure 7. Dune profile showing dune terminology used in report
(4x vertical exaggeration). Location terminology
adapted from Allen, 1968, p. 62.

Relation of Grain Entrainment to Turbulence

The effect of turbulence in a given flow is an important factor in grain entrainment. Local boundary shear stress must be determined from the velocity gradient at the bed and cannot be determined from the slope-depth relationship alone. The apparent shear stress (τ) in turbulent flow is expressed by Streeter (1966, p. 226) as

$$\tau = (\mu + \eta) \frac{dU}{dY} \tag{17}$$

in which μ is the dynamic viscosity, η is the eddy viscosity that depends on the state of the turbulent motion, and dU/dY is the velocity gradient normal to the bed. Intensity of turbulence is important because high turbulent intensities are indicative of large velocity fluctuations and usually indicate large velocity gradients.

McQuivey and Keefer (1969) studied the segregation of magnetite grains from quartz grains on the stoss side of ripples in a small flume and found much larger turbulent intensities over the trough area than over the crestal region of a ripple. Turbulent intensity also decreased with distance from the bed. Measurements were made with a hot-film anemometer. Differences in turbulent shear stress from ripple trough to crest and differences in shear stress required for movement of grains of different densities were considered by McQuivey and Keefer as being important factors in heavy mineral segregation.

Similar results of turbulence measurements are described by Raudkivi (1967, p. 206-207) for experiments conducted by Sheen (1964). Raudkivi describes the greatest turbulent intensities as occurring just downstream from the point of separation (brink line) on a ripple. Intense turbulence is present in the trough area with rapidly decreasing turbulent intensities downstream. Velocity and turbulence profiles were determined by R. S. McQuivey at selected locations for each of the runs of this study. These data are contained in a dissertation by Brady (1971).

Summary

Theoretical considerations of transport of grains with different densities lead to the conclusions that small dense grains are more resistant to tractive movement than larger low density grains and boundary shear is an important parameter in determining the rate of sediment transport.

Different bed forms are produced under different flow conditions with such common bed forms as ripples and dunes formed in the lower flow regime, flat beds formed in an upper flow regime, and washed-out dunes formed in the transition condition.

The turbulent intensity of the flow is large near the bed and decreases with distance from the bed. Much larger turbulent intensities occur in the trough regions of dune beds than occur on the crestal areas with the turbulent intensity decreasing rapidly downstream from the trough area toward the brink line of a dune. Intensity of turbulence is important because high turbulent intensities are indicative of large velocity fluctuations and usually indicate large velocity gradients. The amount of local boundary shear stress is dependent on the local velocity gradient.

EXPERIMENTAL CONDITIONS AND RESULTS OF MATERIALS ANALYSIS

A large recirculating water-sediment flume of rectangular cross-section and dimensions of 61 meters in length, 2.44 meters in width, and 1.22 meters in depth (fig. 8) was used for the series of four

---

Figure 8 (caption on next page) belongs near here

---

experiments. The large size of the flume permits the establishment of flow conditions that approximate flow conditions in a natural channel and eliminates many of the boundary effects that are associated with smaller flumes. The slope of the flume can be changed by use of adjustable screw jacks, and water-sediment discharge can be increased to maximum of approximately 2.5 cubic meters per second. The interior of the flume is surfaced with aluminum having an epoxy coating. A transparent plexiglass section 21.95 meters long is located midway along the left wall of the flume that allows observations to be made of sediment movement.

Adjustable tailgate

61.0 m

Head box

Tail box

Adjustable screw jacks

0.457 m I.D. pipe
0.660 m "   "
0.838 m "   "
Return Pipes

Side contracted orifices

30 HP pump
60 HP   "
120 HP   "

LONGITUDINAL SECTION

2.44 m

1.22 m

Note: Not to scale

Adjustable screw Jacks

Motor

CROSS SECTION
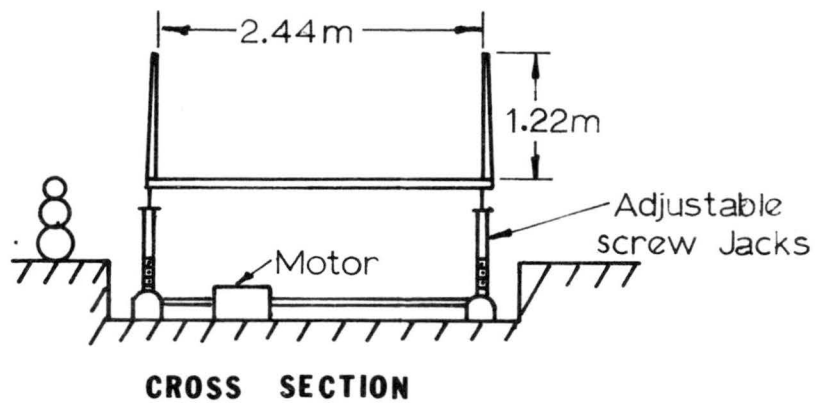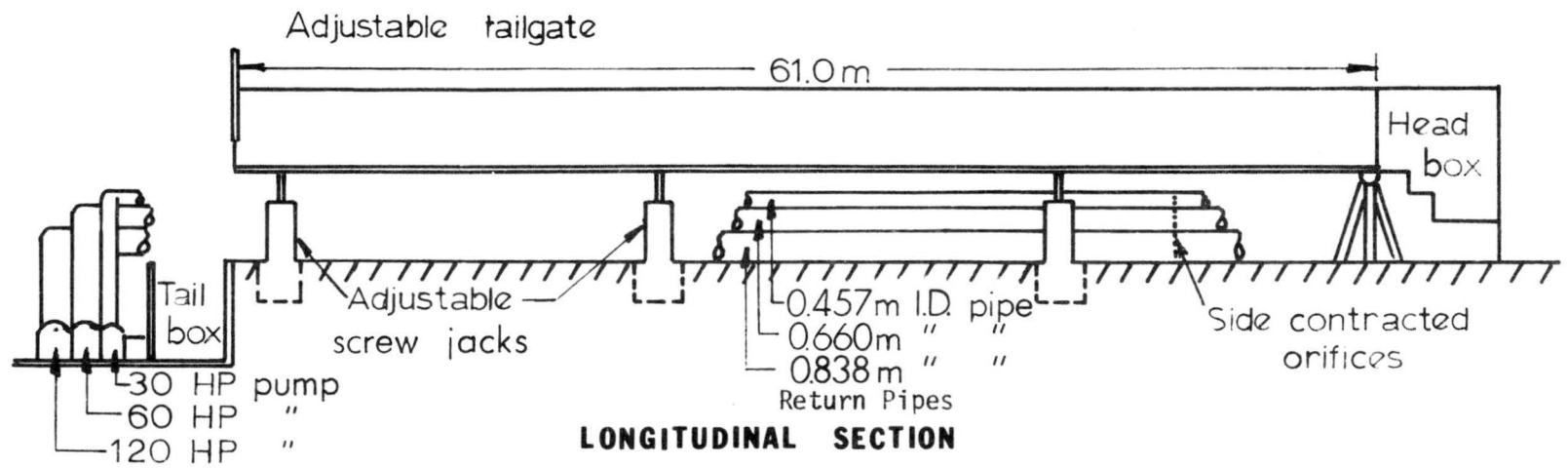
Figure 8.   Schematic diagram of the flume used in the four experimental runs.

Hydraulic Measurements

Near equilibrium conditions were established for each of the flows before sediment and hydraulic data were taken. Equilibrium flow is defined as flow that has established a bed configuration and slope consistent with the fluid, flow, and bed-material characteristics over the working reach of the bed (Simons and Richardson, 1966, p. 3). After equilibrium flow was established for a given experiment, measurements were made of sediment discharge, water-sediment discharge, slope of the water surface and energy grade line, depth, and water temperature. Additional hydraulic parameters were calculated from these basic data. Mean values of significant hydraulic variables are shown in table 2.

Table 2 (p. 45 of ms.) near here

Table 2. Hydraulic variables and parameters of runs.

(cm, centimeters; cu meters/sec, cubic meters per second; dynes/cm^2, dynes per square centimeter)

Run	Bed Form	Energy Slope (x 10^{-3})	Mean Depth (cm)	Water Discharge (cu meters/sec)	Temp. (°C)	Mean Velocity (cm/sec)	Shear Stress (dynes/cm^2)	Froude Number
1	Dunes	1.02	32.9	0.48	20.8	60	33	0.34
2	Dunes	1.06	58.5	1.38	20.9	97	61	0.40
3	Transition	1.22	33.7	0.73	20.7	89	40	0.49
4	Flat bed	1.79	52.8	2.08	21.0	161	93	0.71

Water surface elevations were measured every 1.52 m (meters) along the center line of the flume for several profiles. For each profile a line was fitted to the water surface elevation measurements and their corresponding flume stations by the method of least squares and its slope determined. The mean value of the calculated slopes was taken to be the water-surface slope for the run. By adding the local velocity head, $Q^2/2g(WD)^2$, where Q is discharge, W is channel width, D is water depth, and g is the gravitational constant, to the water-surface elevation at a given measurement point, the elevation of the energy grade line was obtained. The slope of the energy line was determined in a similar manner as the slope of the water surface.

Profiles of the bed and water surfaces along the flume center line were recorded on chart paper by use of a sonic sounder; and from these sounder profiles, the depth of flow was determined. The mean depth of flow (table 2) for the run was determined by averaging the depth values obtained every 1.52 m along each profile.

Water discharge was determined by use of water-air manometers that were connected to calibrated orifice meters located in the three return-flow pipes. Mean discharge for each run was determined from an average of 4 to 20 individual readings. Water temperature was held as constant as possible by use of steam and cold water. The temperature for each run had a fluctuation of less than $\pm$ 1°C (degrees Celsius).

Mean velocity $(\overline{U})$ was calculated by use of the continuity equation

$$\overline{U} = \frac{Q}{A} = \frac{Q}{D \times W} \quad .$$ (18)

Any error in the mean velocity reported would be primarily due to an error in mean depth readings.

The shear stress at the bed (τ_o) and Froude number (F) are both calculated from the above measured variables. The shear stress is defined for a large area as

$$\tau_o = \gamma DS$$ (19)

where γ is specific weight of water and S is the energy slope. The Froude number value is a measure of the effect of gravity on the flow pattern and is defined as

$$F = \frac{\overline{U}}{\sqrt{gD}} \quad .$$ (20)

For a Froude number less than one, a flow is defined as tranquil because the average velocity of the flow is less than the velocity of propagation of small surface waves on the fluid. For a Froude number greater than one, the flow is defined as rapid, for the fluid velocity exceeds the velocity of movement of the small surface waves.

Sediment Analysis

Sediment Characteristics--Sand used in the experiments was obtained
from a conveyance channel of the Rio Grande near Bernardo, New Mexico.
An arkosic sand, it contains approximately 60 percent quartz, 36 percent
feldspars, 3 percent rock fragments, and 1 percent accessory minerals.
Heavy minerals (specific gravity > 2.95) within the bed material com-
prised 1.13 percent by weight and 0.72 percent by volume of the total
bed-material sample. Dark opaque grains, mainly ilmenite and magnetite,
amount to 0.38 percent of the bed-material sample by volume. In addition
to magnetite and ilmenite, other heavy minerals present included
amphiboles, pyroxenes, garnet, zircon, tourmaline, limonite, and
hematite.

Within this report, sediments are referred to as opaque heavy
minerals, consisting of ilmenite and magnetite, and light minerals,
which comprise the remainder of the mineral grains. These two
groupings provided for maximum efficiency in recognition and description
of the segregation characteristics and conditions.

Size Analyses - Total Bed Material--Samples for the bed-material analyses (fig. 9) were obtained from a composite sample of ten vertical cores of the bed. Samples were taken at random locations in the flume

---

Figure 9 (caption on next page) belongs near here

---

after the water had been drained. Median size, as determined by fall diameter using visual accumulation tube (U. S. Inter-Agency Committee on Water Resources, 1958), was 0.286 mm with a geometric standard deviation (σ) (A.S.C.E. Task Committee, 1962, p. 98) of 1.59, where

$$\sigma = \frac{1}{2} \left(\frac{d_{50}}{d_{16}} + \frac{d_{84}}{d_{50}} \right) \quad . \tag{21}$$

A geometric standard deviation, hereafter referred to as sorting with a value of 1.0 refers to a perfectly size-sorted sand while a value of 3.5 or larger refers to a poorly size-sorted sand. Sieve analysis of the bed material showed a median size of 0.285 mm and a sorting (σ) of 1.58 while direct measurement of grains with conversion to the weighted sieve size (See Appendix B for a discussion of technique) showed a median size of 0.287 and a sorting of 1.56.

Weighted median size of the opaque heavy minerals as determined by microscope measurement in the bed material was 0.144 mm with a sorting of 1.49 (Appendix C).
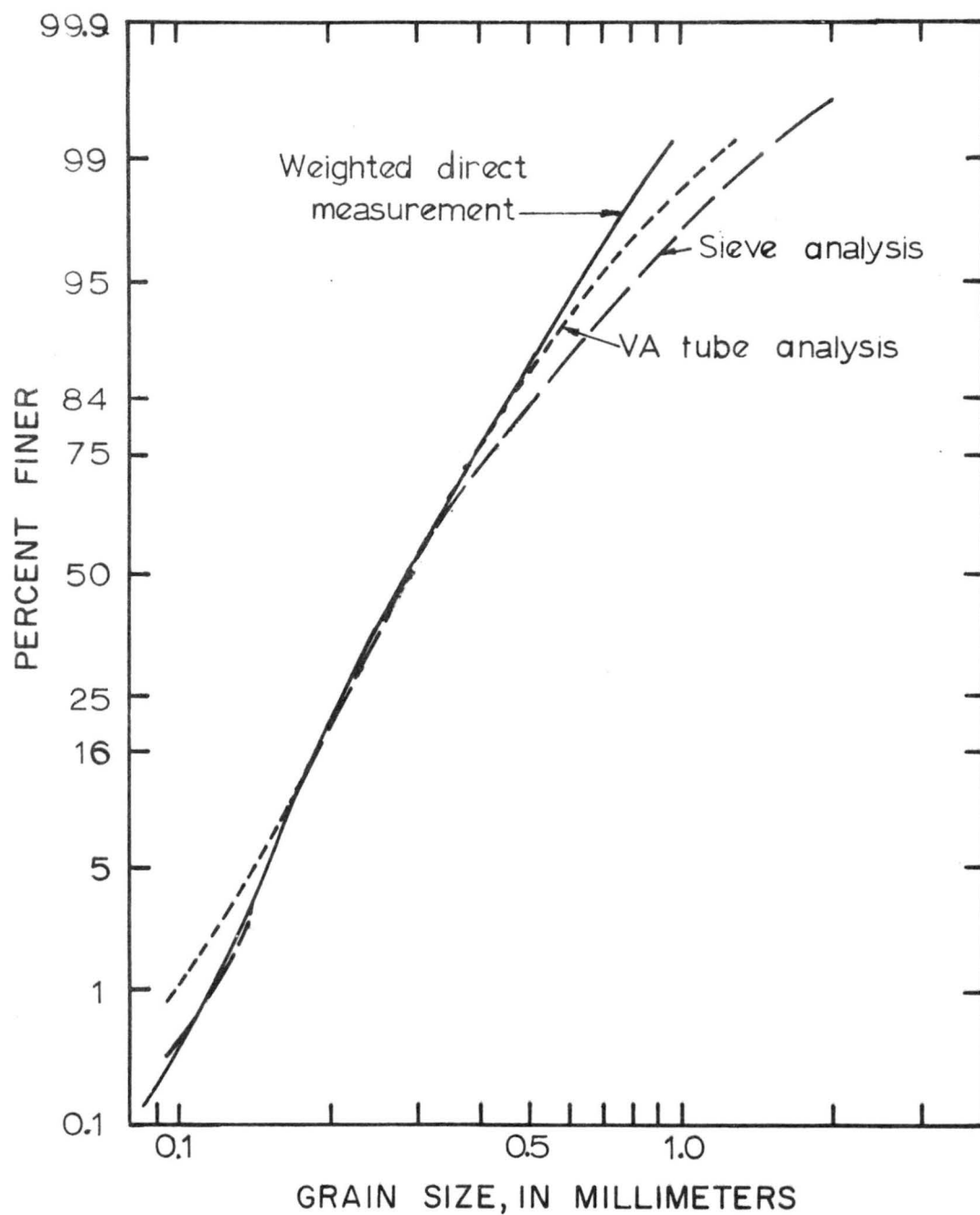
Figure 9. Size distribution curves of sand used in the flume. Curves plotted from analyses by visual accumulation tube, sieves, and weighted direct measurement are shown.

The total-sediment discharge was determined from a width-depth integrated sample of the water sediment mixture collected at the lower end of the flume. Size and gradation of the collected sediment was determined by use of the visual accumulation tube after each sample was dried and split to a workable size.

Size Analyses - Suspended Sediment--Suspended load samples were collected by a siphon with an inside diameter of 0.95 cm (centimeter). Inlet velocity at the siphon nozzle was adjusted to equal the local fluid velocity by changing the total head on the siphon. Local velocities were determined by a modified Ott velocity meter. For dune runs 1 and 2, sediment concentration [mg/ℓ (milligram per liter)] profiles were determined at the trough, bank point, and high on the dune stoss side. Two sediment concentration profiles were measured for the transition run--one in the plane bed reach and one high on the stoss side of one dune. One concentration profile was taken during the flat bed run. Appendix D contains the concentration and size analyses for all suspended sediments analyzed.

Opaque heavy mineral grains were present in the suspended sediment samples from each vertical profile in each of the four runs. Only run 2 had a volume percentage of dark opaque grains approaching that of the bed material. Each of the suspended sediment samples from the runs show the opaque heavy minerals to be distinctly smaller than those of the bed material samples.

Median size of the suspended opaque heavy mineral grains in each run falls below the 20th percentile size determined for the corresponding bed material sample of opaque heavy minerals.

A more complete analysis of the suspended sediment samples has been given by Brady (1971).

Size Analyses - Core Samples--Opaque heavy minerals and light minerals obtained from cores were studied to determine whether differences in size and sorting existed among sediments measured in the different runs. Studies of the opaque heavy mineral grains were concentrated on the dark mineral laminations of runs 2, 3, and 4. Only minor accumulations of opaque heavy minerals were present in run 1, and those were insignificant in thickness and areal distribution when compared to those in the accumulations of runs 2, 3, and 4.

In addition to vertical cores mentioned previously, horizontal core samples were taken from at least two networks across and along the bed following each run. For each network, samples were obtained from the flume centerline and from 0.61 meter from each wall at 1.22 meter intervals along the flume. Total length of each sample network was selected to include the entire length of at least one bed form (average length of the networks was 6.1 meters). Small pits were dug to obtain the samples. Along the wall of each pit a can 6.5 cm in diameter and 12.7 cm in length was inserted horizontally to obtain the horizontal cores. Similar core samples were obtained from large areas of heavy mineral segregation that were missed in the network samples.

Inasmuch as heavy mineral accumulations developed only near the upper surfaces of the bed, it was necessary that the surface sediments be included in the sampling. Therefore, most of these samples were taken in such a way that a small space remained above the sediment surface in the can. Plaster of Paris was poured into this open area and moisture was allowed to evaporate. A chemical soil grout (AM-9, American Cyanamid Co.) was poured into the sample and allowed to harden. Adhesive strength of the grout was controlled to permit easy removal of sand grains from selected areas. The grouted samples were sawed to remove disturbed portions of the core and the sedimentary structures and segregation of minerals studied in the position that they were deposited.

Selection of cores for analysis was based on the presence and location in them of segregated beds of opaque heavy minerals. The method of preparation and a description of the mounting of grains from a lamina within a core sample is described in Appendix B. Complete analyses of size, shape, and sorting are shown in Appendix C, table 5.

In run 2, opaque heavy mineral samples were obtained from topset and foreset beds and from the brink lines of dunes. Samples from run 3 were obtained from topset and foreset beds, and one sample was taken from the flat-bed region. Samples from run 4 were obtained from dark opaque laminae located at the base of and within the flat-bed region. Grain size and sorting for samples shown in Appendix C (table 5) were obtained from direct measurement of 200 individual grains per sample mount.

Size and sorting analyses were determined from grain mounts of light minerals obtained either from light mineral laminae adjacent to or from light minerals present within opaque heavy mineral laminae.

Analysis of variance tests were conducted for the median size, sorting, and shape factor of opaque heavy mineral grains obtained from core samples from runs 2, 3, and 4. The tests are used to determine whether two or more sample means could have been obtained from populations with the same parametric mean with respect to a given variable, or whether the sample means could have been obtained from different populations (Sokal and Rohlf, 1969, p. 175). In this study the analysis of variance tests were conducted to determine if the sediment properties of the opaque heavy minerals in the segregated layers of each run are significantly different in each run. Since the same sediment was used for each run, any significant differences in the sediment properties between runs must be due to the effect of the different flows on the grains.

Data used for the analysis of variance tests were obtained from laminae of dark opaque minerals in the core samples (Appendix C, table 5). A more complete presentation of these results has been given by Brady, (1971, p. 44).

The results of the tests on the median grain diameter and the grain shape factor of opaque heavy mineral grains showed that no differences existed among runs at the 5 percent level of significance. A significant difference, however, did exist in the sorting among runs at the 1 percent level. An a posteriori SNK test (Sokal and Rohlf, 1969, p. 239-246) of the sorting means of the three runs was conducted to determine which run was significantly different from the others. Results of the SNK show that the mean sorting value of the opaque heavy mineral samples in run 4 is significantly larger than the other two runs at the 1 percent significance level.

The median diameter and sorting for light mineral samples that were obtained adjacent to and within the opaque heavy mineral laminae also were tested by analysis of variance tests (sorting and median diameter values of the samples are listed in Appendix C, table 6). The tests show that no difference in sorting of light minerals existed between runs 2, 3, and 4; but, a significant difference did exist at the 5 percent level between the median diameter of the samples. Results of these tests should indicate whether a given flow had an effect on the properties of light mineral grains that were closely associated with opaque heavy mineral grains that differed significantly from the other flows.

A SNK test of the mean of the sample median grain sizes for each of the three runs showed that no significant difference existed between the three runs. However, a SNK test for uneven sample sizes, such as was used for runs 2, 3, and 4, does not provide sufficient sensitivity to determine which run differed significantly from the other two in its effect on sample median size.

EXPERIMENTAL RESULTS

Summary of Bed Form and Opaque Heavy Mineral Segregating Characteristics

Four different flow conditions were observed in this study (table 2); and based on the terminology of Simons and Richardson (1966), two runs were made in the lower flow regime, one run in the upper flow regime, and one run in transition between the upper and lower regimes. A bed configuration consisting of dunes (lower flow regime) existed in runs 1 and 2. Transition bed forms of long profile dunes and a near flat-bed condition existed in run 3, while run 4 consisted entirely of a flat bed formed in the upper flow regime. Average lengths (L), heights (H) and length/height ratios for the dunes of different runs measured from sonic sounder charts are listed in table 3.

Table 3 (p. 56 of ms.) near here

Only thin accumulations of opaque heavy minerals covering small areas were present at the surface of bed forms produced by run 1. All other runs resulted in accumulations of large areas and appreciable thicknesses of opaque heavy minerals associated with the bed forms.

Table 3. Mean dune size (with standard deviations) measured by sonic sounder.

(cm, centimeters; m, meters)

Run	Number of Dunes Measured	Height* (cm)	Length** (m)	L/H Ratio
1	115	10.2 ± 4.9	1.63 ± 0.66	18.2 ± 8.7
2	28	30.0 ± 13.2	7.24 ± 4.67	26.3 ± 15.0
3	46	12.3 ± 6.8	5.66 ± 2.48	46.6 ± 29.6

* Dune height (H) determined by maximum vertical distance between the trough point and the summit point of the dune as measured along center line of the flume.

**Dune length (L) was determined from the low trough point between dunes to the next trough point downstream as measured along the center line of the flume.

Dune Bed Forms (Run 1)--Dunes in run 1 were formed under conditions of a low shear stress at the bed (table 2). In profile the dunes of run 1 were generally triangular in shape with the crest line of the dune coinciding with the dune brink line. Topset beds occurred on only a few dunes in run 1. The average angle of inclination of the foreset beds in run 1 was 32.4° with a standard deviation of 2.3°. Configuration of the dunes forming the bed surface (figure 10A) can best be described as linguoid. Rates of movement of the dunes ranged from 0.6 to 1.0 meter per hour.

Figure 10 (caption on next page) belongs near here

Accumulations of opaque heavy minerals associated with the dunes were limited to small, very thin ripple-form accumulations on the stoss slopes of the dunes (figure 10B). The small thin accumulations of opaque heavy minerals appear to develop just downstream of the re-attachment point (the location where the flow impedes on the back of the downstream dune after it has passed over the upstream dune front) and migrate up the dune stoss slope. No accumulations of opaque heavy minerals were observed in the foreset beds.
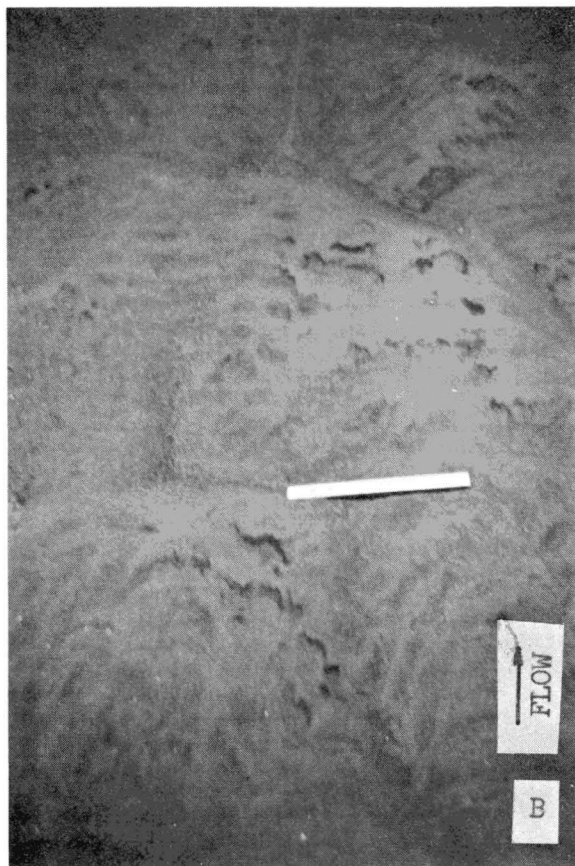
Figure 10. Dune bed configuration and opaque heavy mineral
accumulations at the bed surface following run 1.
(A) Dune-bed configuration, (B) Stoss slopes of
dunes showing small areas of accumulated opaque
heavy minerals (length of rule is 30.5 cm).

Dune Bed Forms (Run 2)--Dunes formed by flow conditions in run 2 (table 2) were longer and higher than dunes produced by the other runs. Distances between brink lines and crest lines of dunes commonly ranged from 25 to 110 cm, and averaged 60 cm. Topset beds, which are generally composed of rather fine material, were present on most dunes with the total thickness of topsets ranging up to 3 cm. Foreset beds of the deposits in run 2 showed an average dip of 29.2° and a standard deviation of 3.1°. Generally the inclination angles of the foreset beds ranged from 28° to 32° but some low bed angles of 21° to 23° existed that indicate unstable conditions in the dune development. Dune fronts in run 2 were sinuous across the width of the flume (figure 11, 12), and rates of movement of the dunes down the flume

Figures 11,12 (captions on following pages) belong near here

(based on successive brink line locations) ranged from 1.5 to 3.4 meters per hour.
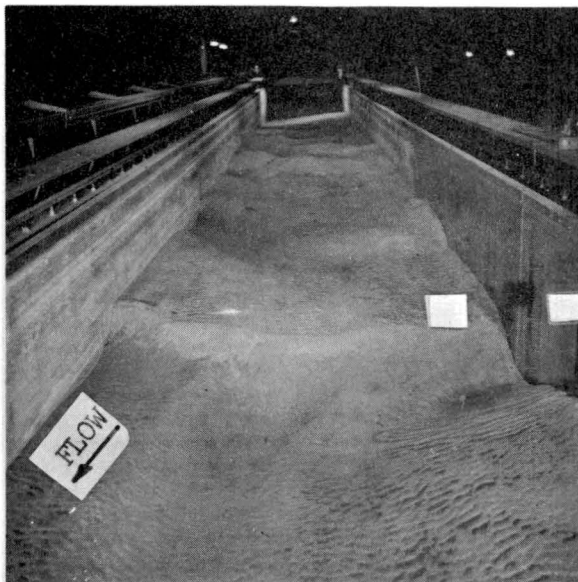
Figure 11. Dune-bed configuration of run 2. Figure 12 is
a close view of the large dune in the center
of the photograph on which the white square is
located.
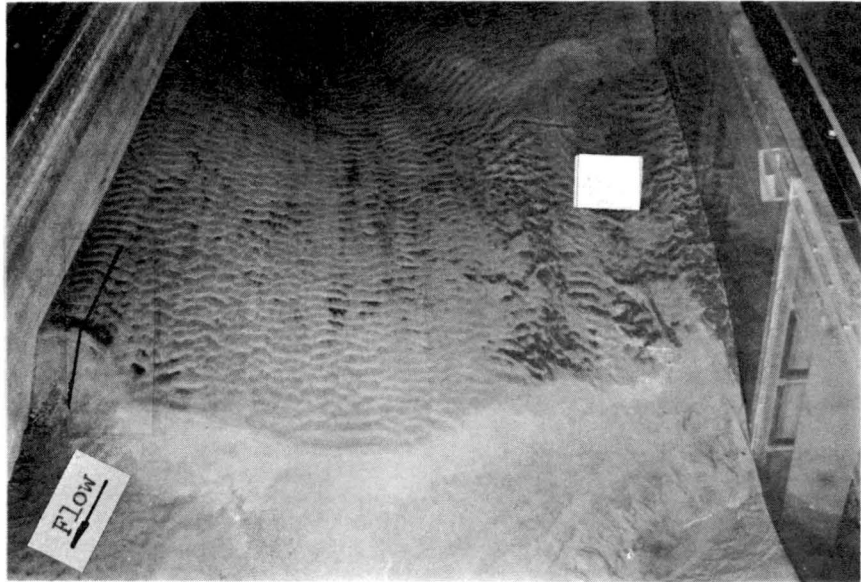
Figure 12. Accumulations of dark opaque heavy minerals on the
upstream sides of dunes (run 2). Location of cut-
away view of dune (figure 14) is shown by the line
near the flume wall on left side of photograph.
The ripple surface that is shown on the dune is due
to abrupt changes on hydraulic flow conditions that
occurred when the flume was shut down at the end of
the run. Segregation of the heavy minerals was not
formed by shutdown of the flume.

Accumulations of opaque heavy minerals were associated with the dunes (figure 13) and commonly were present as:

Figure 13 (caption on next page) belongs near here

---

1. Accumulations of opaque heavy minerals on the dune stoss slopes that formed thin ripple-form accumulations and very thin, almost sheet-like accumulations. The thin ripple accumulations resembled those shown in figure 10B and were very common on the dune stoss slopes. The ripple accumulations appear to have originated on the lower part of the dune stoss slope and migrated up the dune. Thin sheet-like accumulations of the opaque heavy minerals such as shown in figure 12 were present on many dune stoss slopes.
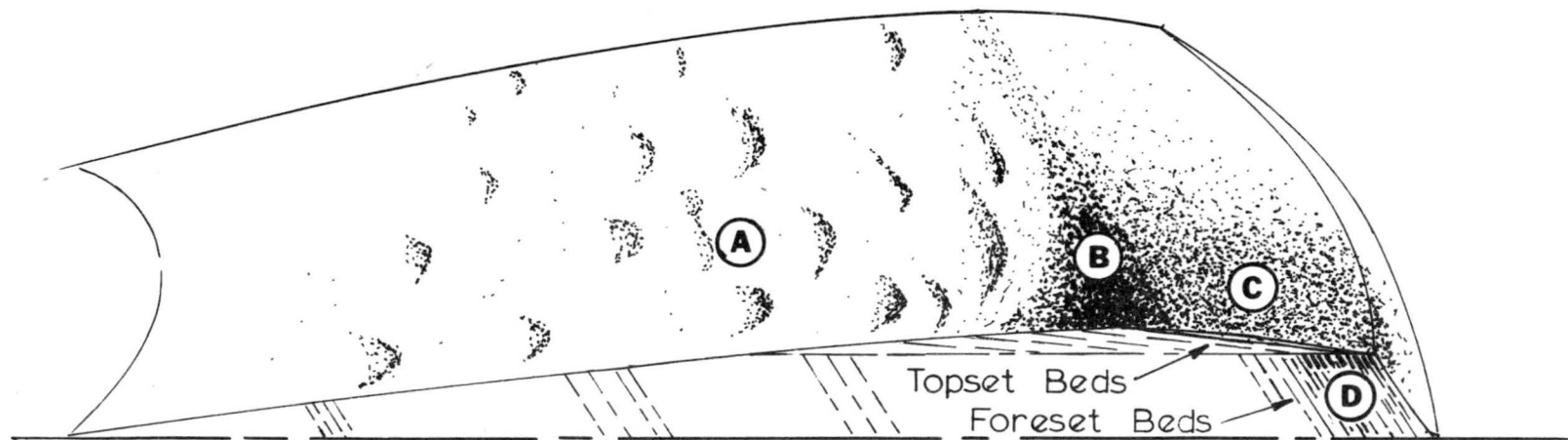
Figure 13. Generalized view and cut-away of a dune showing structures and location of different types of opaque heavy mineral accumulations: (A) Thin ripple-form accumulations on stoss slope, (B) Crestal region accumulation, (C) Region between the crest line and brink line where accumulations occur, and (D) Accumulations in foreset beds (3x vertical exaggeration).

2. Thick accumulations of opaque heavy minerals that formed on the high portions of the dune associated with the dune crest area. These accumulations formed the thickest beds of opaque heavy mineral accumulations observed and the beds were nearly 100 percent efficient in segregation of opaque heavy minerals. Observations made through the plexiglass wall of the flume during the flow showed that the opaque heavy mineral accumulations formed on the highest portion of the dune (in dune profile). The accumulation as a whole moved downstream at a rate approximately equal to the rate of movement of the dune. Scour occurred periodically both upstream and downstream of the heavy mineral area. If degradation immediately downstream of the heavy mineral area reached approximately 1 to 2 cm below the high point of the accumulation, a large amount of the heavy minerals was transported from the accumulation by suspended and tractive movement which resulted in a heavy mineral lamina.

3. Accumulations of opaque heavy minerals that were deposited between the dune crest line and the brink line. These deposits, derived from the thick crest area accumulation of opaque heavy minerals, formed part of the topset beds of the dune. An example of numerous opaque heavy mineral laminae in the topset beds is shown in figure 14B.

Figure 14 (caption on next page) belongs near here
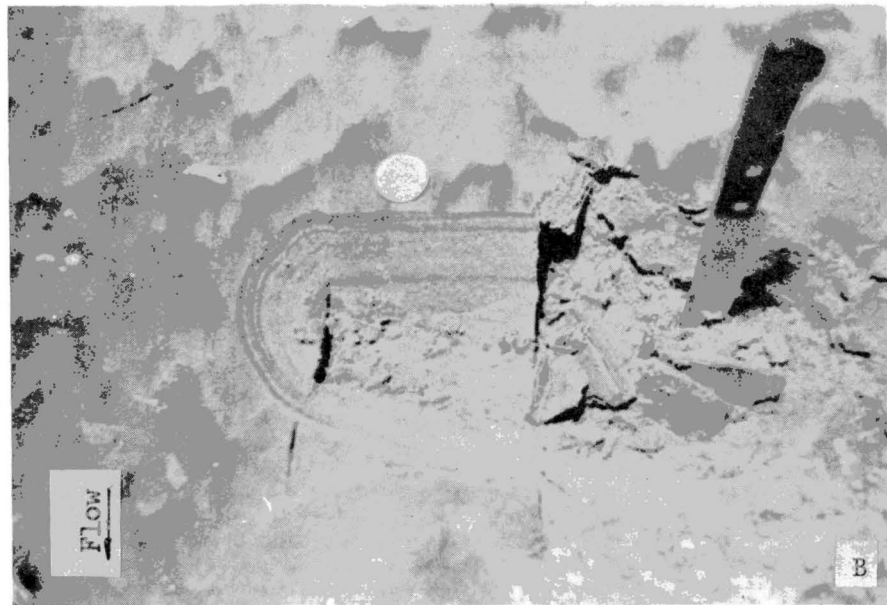
Figure 14. Opaque heavy mineral accumulations in foreset and topset beds of dunes formed in run 2. (A) Cut-away part of dune shown in figure 12 showing accumulation of opaque heavy minerals (dark beds) in the foreset beds (can diameter is 6.5 cm), (B) Segregation of opaque heavy mineral grains in topset laminations.

4. Accumulations of opaque heavy minerals at the brink point
and deposited on the slip face of the dune. These deposits formed
dark laminae in the foreset beds like those shown in figure 11A. The
concentrated opaque heavy mineral layers did not extend down the
foreset beds more than 8 cm (total slip face length on the dunes
commonly was between 20 and 30 cm) and a decrease in concentration
of heavy minerals occurred with increased distance down the bedding
plane from the brink line. Losses of opaque heavy minerals from the
topset beds occurred by tractive and suspended transport over the
brink point.

Transition Bed Forms (Run 3)--During the run the bed forms

alternated between large dunes (figure 15A, 15B) and a near flat-bed

condition (very long profile dune). The near flat-bed condition

---

Figure 15 (caption on next page) belongs near here

---

of the run differed from a true flat bed because at no time did the

flat bed extend over the entire length of the flume. In addition,

the near flat-bed condition differed from the flat bed of run 4

by having a slip face on its downstream edge as well as slight form

irregularities on its surface. Dunes associated with run 3 had a

much larger length to height ratio than the dunes of runs 1 and 2.

The distance from the crest line to the brink line for the dunes

of run 3 commonly ranged from 15-85 cm with a mean distance of 53 cm.

In some cases the distance was as large as 2.5 meters. Topset beds of

fine material were present on virtually all the dunes. Dune fronts

were sinuous across the flume as shown in figures 15A and 15B. Angles

of inclination of foreset beds averaged 28.6° with a standard deviation

of 3.2°. Several foreset dip values of 21° to 23° indicated local

conditions of unstable deposition. Rates of movement of the dune

fronts ranged from 2.7 to 4 meters per hour.

Figure 15. Bed configuration and opaque heavy mineral accumulation
at the bed surface formed during run 3. (A) Dune region
of transition flow, (B) Close-up view of dunes showing
opaque heavy mineral segregation on the dune stoss slopes.
Ripples present on the dunes were not present during the
run but were formed as the result of abrupt changes in
flow conditions during flume shut down.

Opaque heavy mineral accumulations were common in association with the transition bed forms. Their occurrences can be classified as follows:

1. Thin but widespread accumulations near the base of flat beds, just above foresets formed with or as part of dunes deposited earlier.

2. Thin laminae of concentrated opaque heavy minerals within the flat beds. These laminae were usually thinner than the opaque heavy mineral beds at the base of the flat bedded sediments.

3. Accumulations associated with the dune phase of the transition bed forms. They were basically the same as those associated with the dunes of run 2, namely:

    a. Thin accumulations in ripple-form and sheet-like accumulations that advance up the stoss side of dunes.

    b. Thick accumulations that were commonly present along the crestal region of the dune (figure 16A, 16B).

Figure 16 (caption on next page) belongs near here
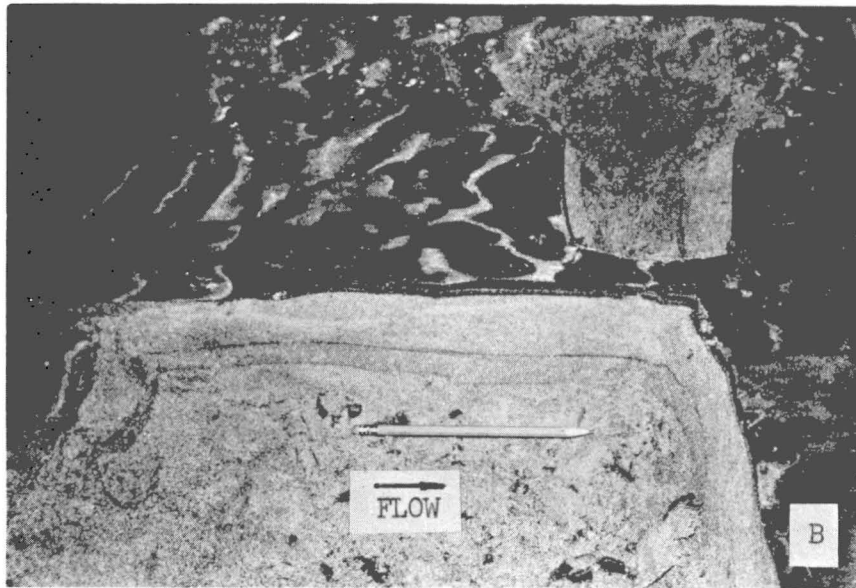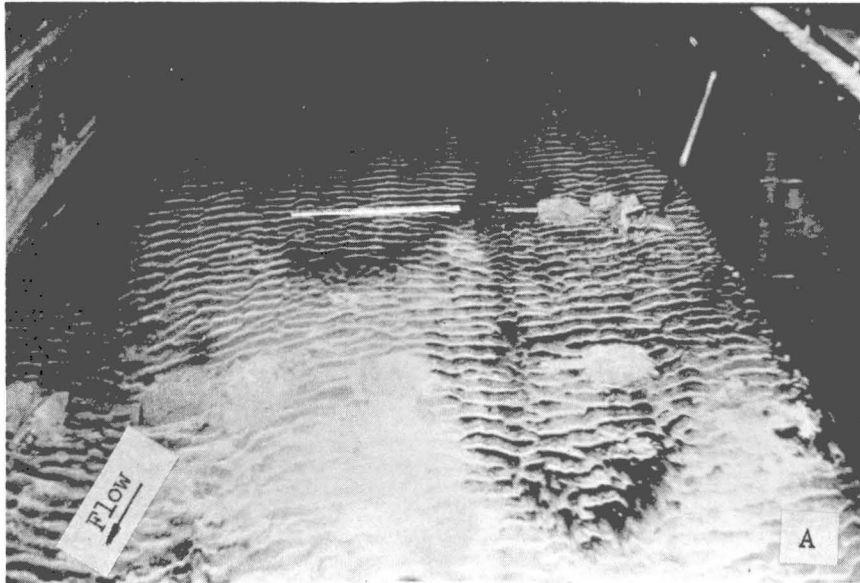
Figure 16. Accumulations of opaque heavy minerals formed along the
crestal region of a dune (run 3). (A) Accumulation on
the crestal region of a long dune in the transition flow,
(B) Exposed topset beds (located at the right side of the
71-cm rule, fig. A) showing the thick accumulation.

c. Accumulations that were present downstream from the
crest line and extending to the brink line (figure 17A,
17B). In several dunes opaque heavy mineral

Figure 17 (caption on next page) belongs near here

---

segregation was observed in the foreset beds as shown
in figure 17A.

d. Thick accumulations were often present in the topset
beds. These deposits resulted from burial of surface
accumulations.
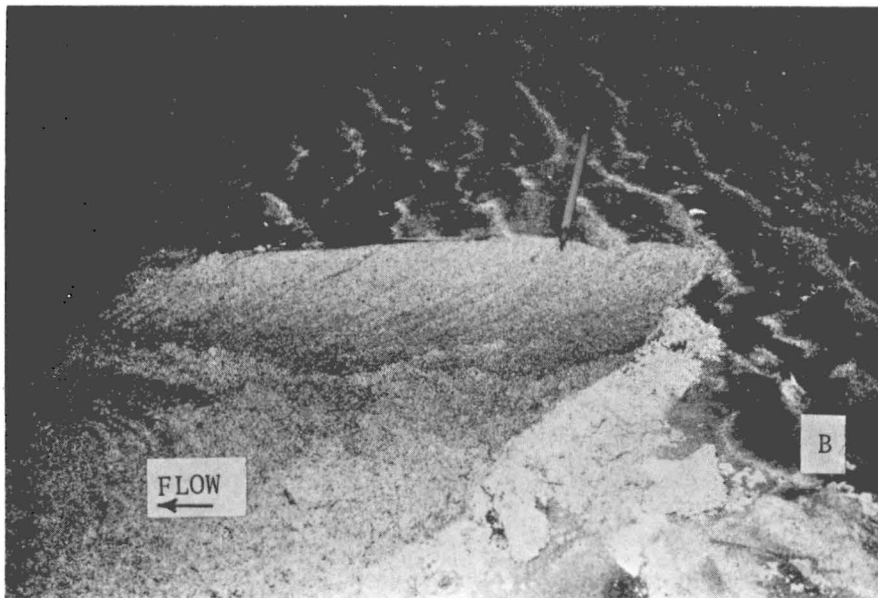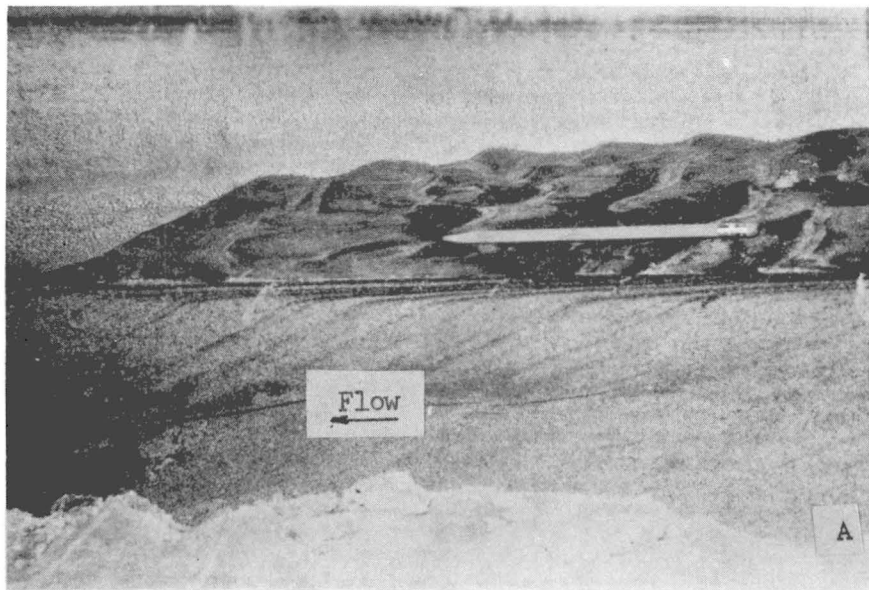
Figure 17. Opaque heavy mineral accumulations formed in topset and
foreset beds during run 3. (A) Opaque heavy minerals
in dark laminae of topset beds near the brink line and
in the foreset beds after passing over the brink point,
(B) Foreset beds with very few opaque heavy minerals
present, but a large amount of opaque heavy minerals are
present in the thin topset beds.

72

Bed Forms of Moving Flat-Bed Conditions (Run 4)--The flow that produced the flat beds of run 4 had the highest shear stress and Froude number of any of the four runs. Under equilibrium flow the sediment bed had an essentially featureless surface (figure 18). The bed elevation at any point departed only a few centimeters from the

---

Figure 18 (caption on next page) belongs near here

---

mean elevation. A study of bed surface elevation fluctuations at one location during the equilibrium flow showed a maximum fluctuation of only 1.8 cm in a 12 hour period. Studies by Guy, Simons, and Richardson (1966, p. 24, 29) show vertical fluctuations with time of flat-bed surfaces during several runs as ranging from 1 to 3 cm. Bedding structures were all flat lying and covered pre-existing bed forms. Generally the material in the flat lying deposits was finer than the material in the pre-existing foreset beds. Total thickness of the flat beds in the run was usually less than 3 cm.

Of the four runs studied in detail, total sediment concentrations in the total-load and suspended-load samples were by far the largest in run 4.

Figure 18. Flat-bed surface formed by run 4. Ripples at the surface were due to shut down of the flume.

Opaque heavy mineral accumulations were common in the flat-bed run and accumulations of the heavy minerals were present at the base of and within the flat beds over virtually the entire flume area (figure 19). The individual beds, however, tended to lense out within a few

---

Figure 19 (caption on next page) belongs near here

---

meters. Accumulations were often the thickest and most widespread at or near the base of the flat beds. In run 4 no opaque heavy mineral accumulations were present at bed surface.
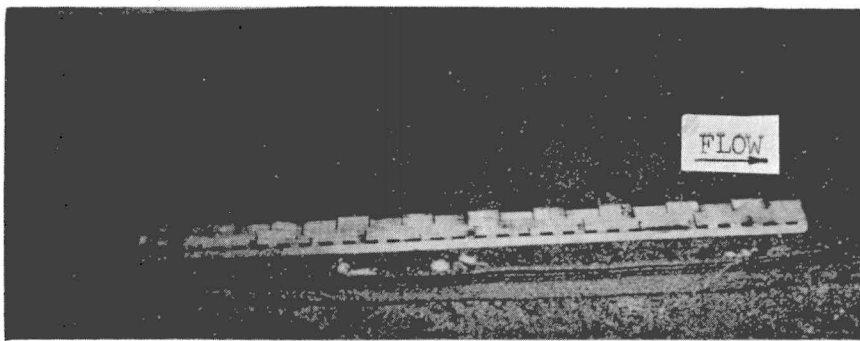
Figure 19. Profile of flat-bed structure showing segregation
of opaque heavy minerals (dark beds) in flat-lying
beds. Lower dark mineral bed is directly overlying
foreset beds of an earlier run. Wavy appearance of
the dark laminae in the photograph is due to an
irregular cross-section cut. The rule is 71 cm in
length.

Relation of Fall Velocities of Dark Opaque and Light Density Grains

Samples of light minerals obtained from laminae adjacent to or located within laminae having a high concentration of opaque heavy minerals were studied to examine relation of fall velocities of associated light and heavy mineral grains.

In order to compare fall velocities, a graph (figure 20) relating

---

Figure 20 (caption on next page) belongs near here

---

sieve size to fall velocity for grains with a shape factor of 0.7 and with specific gravities of 2.65 and 5.0 was plotted from data reported by the U. S. Inter-Agency Committee on Water Resources (1957). Values of fall velocities for the d_{16}, d_{50}, and d_{84} grain sizes were determined from figure 20 using the samples described in Appendix C, tables 5 and 6. These fall velocity values have been tabulated by Brady (1971, p. 112). Fall velocity relations between opaque heavy mineral grains and light mineral grains of the bed material sample and the average of all the core samples are shown in figure 20. Using the range between the 16th and 84th percentiles of the opaque heavy mineral grains and the light mineral grains for the sampled laminae in the core samples, the average for the core samples shows 78 percent of the light mineral grains having fall velocities within the same range as 80 percent of the opaque heavy mineral grains. For the bed material samples, 74 percent of the light mineral grains had fall velocities equal to 78 percent of the opaque heavy mineral grains.
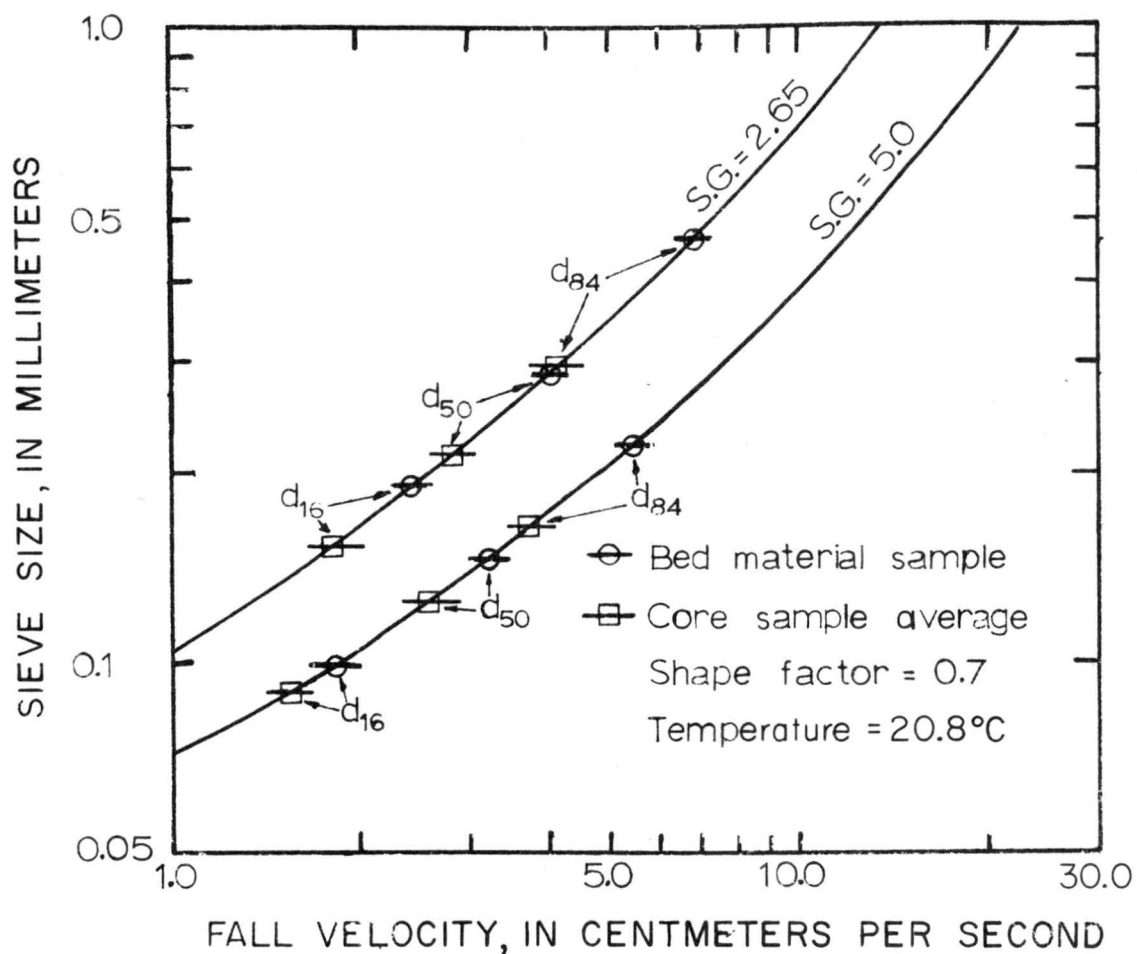
Figure 20. Fall velocity relationship of light mineral grains to opaque heavy mineral grains obtained from the bed material sample and core samples of runs 2, 3, and 4.

Median fall velocity values of the opaque heavy minerals and the median fall velocities of light minerals sampled adjacent to (18 samples) or within (5 samples) the opaque heavy mineral laminae have a correlation coefficient of .369 (figure 21) a value that suggests

---

Figure 21 (caption on next page) belongs near here

---

no correlation exists. The lack of correlation for medians of fall velocities between the two mineral groups shows that the median fall velocity of one group is not a predictor of the median fall velocity of the other group. With large number of grains having equivalent fall velocities existing for the two mineral groups in adjacent laminae, the lack of correlation for mean fall velocities of the opaque heavy minerals and light minerals suggests that other factors were much more important for the occurrence of local sorting.
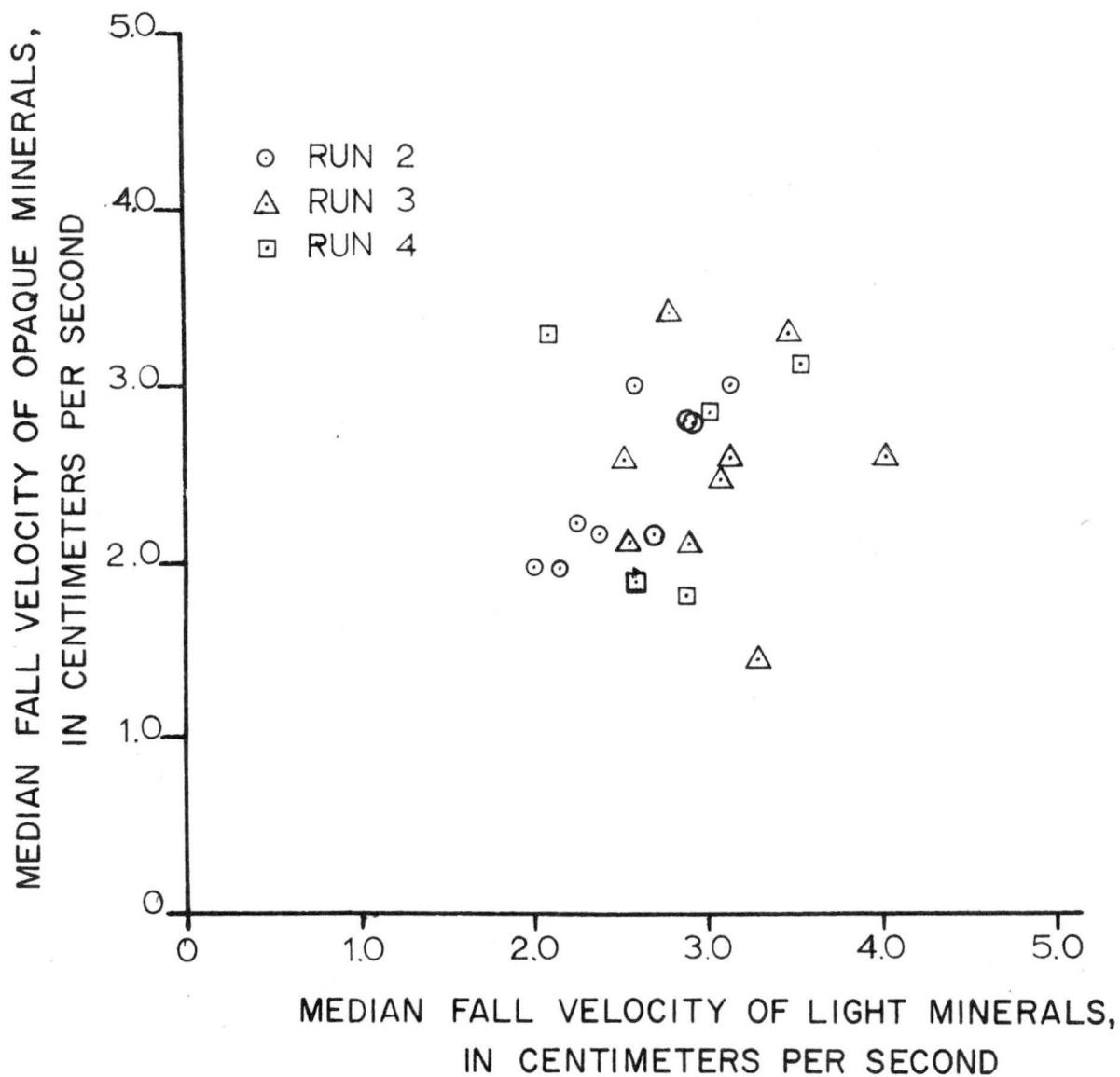
Figure 21. Plot of median fall velocities of opaque heavy mineral grains and light mineral grains.

Relation of Grain Entrainment to Critical Shear Stress
and Grain Size

Based on the Shields' diagram (figure 5) one can develop the relation of critical shear to grain size for grains of different densities.

Such a series of curves was developed by Grigg and Rathbun (1969, p. 79). Two curves similar to those constructed by Grigg and Rathbun are plotted in figure 22 for grains of 5.0 and 2.65 specific gravities.

Figure 22 (caption on next page) belongs near here

The range between the 16th and 84th percentiles of the opaque heavy mineral grains and the light mineral grains of the bed material and the average values for the sampled laminae in the core samples from runs 2, 3, and 4 are plotted in figure 22 to show that a large difference exists in critical shear between the two mineral groups. This difference in critical shear indicates that movement of the quartz and feldspar grains from sands in this study would occur much more readily than movement of the magnetite and ilmenite grains.
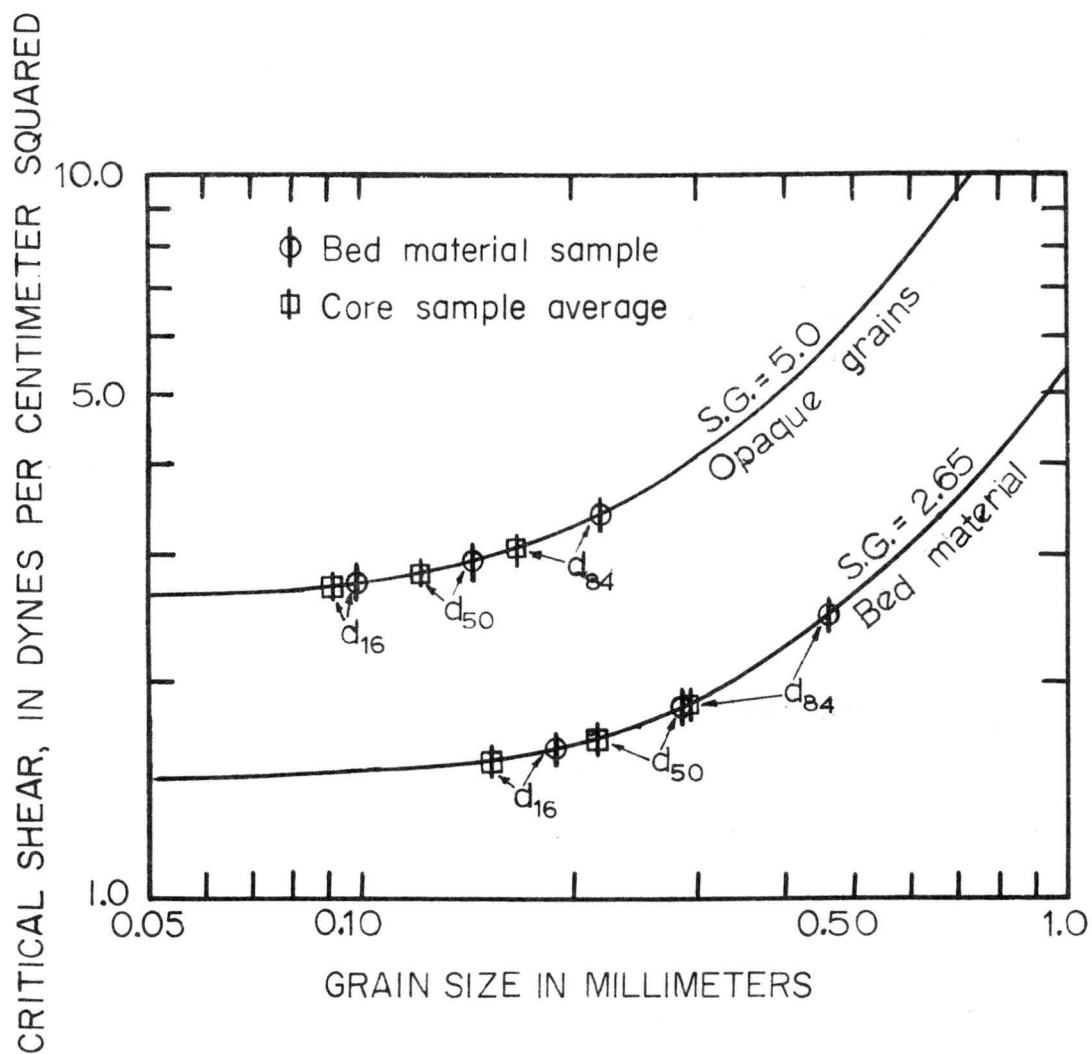
Figure 22. Critical shear relationship of light minerals to opaque heavy minerals for the bed material and core samples.

Figure 22 is based directly on Shields' diagram. The data on
this diagram was obtained by use of particles which moved over a bed
that consists of particles of the same size. The effect of differences
in size of the moving and stationary particles has been discussed on
pages 11 and 12. By use of figure 1 one can qualitatively adjust figure
22 so that it is more applicable to the flume situation. For example
figure 1 indicates that the resistance of a 0.1 mm particle attempting
to move on a bed of 0.2 mm particles is underestimated on figure 22 by
as much as a factor of 3. Once a small magnetite or ilmenite grain is
deposited on a bed of large quartz and feldspar grains, it is extremely
difficult for the flow to move it again.

The resistance of a 0.4 mm particle resting on a bed composed of
0.2 mm particles is over estimated on figure 22 by perhaps a factor of
2. The flow will quickly remove a large quartz or feldspar particle
from a place on a bed which is composed of small dense grains.

In addition to effects discussed on page 11 and above, distinct
differences in physical size between grains also leads to a "hiding
factor," or a shielding of the smaller grains from the flow by the
larger grains. Einstein and Chien (1953) have discussed the "hiding
factor." They found that the effective shear required to transport
very small particles over a bed composed of large particles was
significantly larger than that required to transport them over a
bed composed of very small particles.

The above discussion suggests that the slope of the lines in figure 22 may actually be negative when the bed is composed of a poorly sorted material in the size range of interest here. An experiment was conducted in order to determine what effect the sorting of the bed material might have on a particle's resistance to motion. A flat bed of quartz sand (d_{50} = 0.280 mm, σ = 1.50) was placed over a 94 cm section of a flume 20 cm deep, 20 cm wide, and 10 meters long. The bed roughness for a section 6 meters long upstream of the sand bed was similar to that on the sand bed. The flow was started with a velocity insufficient to move any of the bed material and the velocity was gradually increased. During the velocity increase the water depth was held constant at 3.5 cm, while the slope of the water surface remained parallel to that of the bed. The velocity was increased slightly each 24 hours for six days. The total material transported from the test section during each day (run) was collected and sieved.

Results of this experiment (table 4) show that little sediment

---

Table 4 (p. 86 of ms.) near here

---

was eroded during the first 5 runs. Ripples developed and a considerable
amount of sediment was eroded during the last run. The erosion during
run F occurred mainly at a few isolated scour holes which were several
millimeters deep.

The selectivity with which the flow transported a particular
size fraction of the bed material can be determined by computing the
ratio of the percent of that size fraction in the material transported
out of the test section to the percent of the size fraction which was
available for transport. This ratio will be called the transport ratio.
Transport ratios which are greater than one indicate size fractions
which are readily transported or which have a low resistance to motion.
If a particle's resistance to motion was correctly represented by
figure 22, one would expect the transport ratio to decrease continu-
ously with increasing particle size.

By assuming that a representative sample of the bed material
was available for transport on the bed surface at the beginning of run
A, the transport ratios for each size class and run were computed from
the data given in table 4. Except for run A which didn't transport
any sediment larger than 0.707 mm, the transport ratios were larger
than one for all grain sizes greater than 0.35 mm. The value of the
transport ratio increased consistantly with grain size in the range
0.25 to 1.0 mm.

Table 4. Results of a resistance to motion experiment using
a poorly sorted quartz bed material

Run	Size, in millimeters								Total
	0-.062	0.062-.125	0.125-.177	0.177-.250	0.250-.350	0.350-.500	0.500-.707	0.707-∞	
(a) Weight (grams) of material eroded during the run									
A	0.0006	0.0089	0.0126	0.0132	0.0157	0.0285	0.0010	0	0.0805
B	0.0007	0.0067	0.0100	0.0089	0.0098	0.0180	0.0109	0.0010	0.0660
C	0.0016	0.0110	0.0147	0.0109	0.0075	0.0136	0.0146	0.0017	0.0756
D	0.0013	0.0104	0.0235	0.0387	0.0528	0.0784	0.0554	0.0012	0.2617
E	0.0016	0.0111	0.0133	0.0236	0.0827	0.2505	0.2033	0.0051	0.5912
F	0.000	0.019	0.594	3.221	8.106	11.106	4.085	0.057	27.188
Total	0.006	0.067	0.668	3.316	8.275	11.495	4.370	0.066	28.263
(b) Percent of total eroded material									
---	.02	.24	2.37	11.7	29.3	40.6	15.5	.23	---
(c) Percent of bed material									
---	.2	4.9	11.0	22.8	33.2	22.2	5.6	0.05	---
(d) Ratio (Percent eroded)/(Percent in bed)									
---	.1	.05	.22	.52	.88	1.8	2.8	5	---

It is suspected that some sorting of the bed material occurred at the bed surface as a result of the placement of the bed and that this sorting affected the resulting transport ratios of the smaller grain sizes during the first five runs. Therefore, no significance is attached to the transport ratios of the finer sizes for the first five runs.

Ripples were developing during run F and the major portion of the scour occurred at a few scour holes which became several milli- meters deep. Because of this erosion pattern, it is believed that the size distribution of the material which was available for transport was nearly the same as the size distribution of the total bed material and that the computed transport ratios for run F accurately represent the resistance to motion of the particles.

The transport ratios for run F increased consistently with particle size throughout the entire range of particle sizes. There- fore, it is concluded that the resistance to motion of sand grains decreases with increasing grain size when the transport is occurring over a poorly sorted bed. There obviously must be some maximum size above which this relation is no longer true. The data presented in table 4 indicate that this maximum size is larger than 1.0 mm.

These results indicate, as was suggested by the consideration of figure 1, that figure 22 does not correctly represent the variation of the resistance to motion with particle size for material being trans- ported over a poorly sorted bed material. The resistance to motion should decrease, rather than increase, with increasing particle size for particle sizes within the range of 0.05 to 1.0 mm.

The median size of the total load transported in these small flume experimental runs made at the point of initiation of grain movement was larger than the median size of the bed material, whereas the median size of the total transport load samples from the large flume runs were smaller than that of the bed material. In natural streams, total load samples almost always have smaller median sizes than the bed material of the stream (Carl F. Nordin, personal communication, April, 1971).

Smaller particles are, of course, more easily entrained and carried in suspension by the flow and the suspended load always has a smaller median size than does the total load. It is usually impossible to determine the size distribution of the entire suspended load so that the true size distribution of the bed load is seldom known either in the field or in the laboratory.

In addition, the median size of the bed material tends to increase with distance below the mean bed elevation for fully developed bed forms. As a consequence the coarser particles tend to be exposed to the flow and available for transport at less frequent intervals than are the finer particles which tend to be deposited at higher elevations in the bed. This factor would tend to account for a higher transport rate of small particles even though their resistance to motion along the bed was greater than that of larger particles.

The small flume experiment shows that a marked "hiding effect" does exist for a poorly sorted bed material and this result is consistent with flume and field data. When small grains form only a small part of the surface material such as the small opaque mineral grains in this study prior to segregation, the selective removal by the flow of larger less dense grains can become an important factor to their segregation.

Heavy Mineral Transport and Deposition in a Flat-Bed Flow

Accumulations of dark opaque minerals were widespread in the flat-bed runs (Run 4). The accumulations of opaque heavy minerals at the base of the flat-bedded sands suggested that the heavy minerals concentrated at the base of the tractive load during degradation and were the first deposited during aggradation. To test the above hypothesis, a study was made of the transport of heavy minerals relative to time under equilibrium hydraulic conditions. The small recirculating water-sediment flume (20 cm deep, 20 cm wide, and 10 m long) was used in the experiment with a sand bed of the same Rio Grande sand that was used in the large flume runs. The sand bed was thoroughly mixed after the flow was started. Mixing of the sand provided maximum possible exposure of heavy minerals to the flow. The run, which lasted for 47 hours, was started just after the mixing of the sand.

Hydraulic conditions necessary to form the flat bed were held as constant as possible throughout the run. Average discharge for the run was 10.98 liters per second with an average water depth of 7.36 cm. Water surface slope was .0045, and the average temperature was 16.9°C. Total load samples containing 80 to 135 grams of sediment were collected at close time intervals (15 minutes) early in the study with increasingly longer time intervals (up to 7 hours) as the study progressed. Total load concentrations for the study averaged 2699 mg/ℓ.

Sediment from the total load sample that passed the 60 mesh (.25 mm) sieve was retained for magnetite separation. Magnetite less than .25 mm was used in this study as the marker mineral because of the ease of separation of magnetite and because 88 percent of the dark opaque minerals of the bed material sample were finer than .25 mm. A strong hand magnet was used to separate the magnetite grains from the sample and the percentage of magnetite in the sand passing the 60 mesh sieve was calculated. Results of these percentage plots relative to time (figure 23) confirm the hypothesis that in a flat-bed flow under equilibrium conditions there is a decreasing volume of transport of heavy minerals with increasing time of transport.

Figure 23 (caption on next page) belongs near here
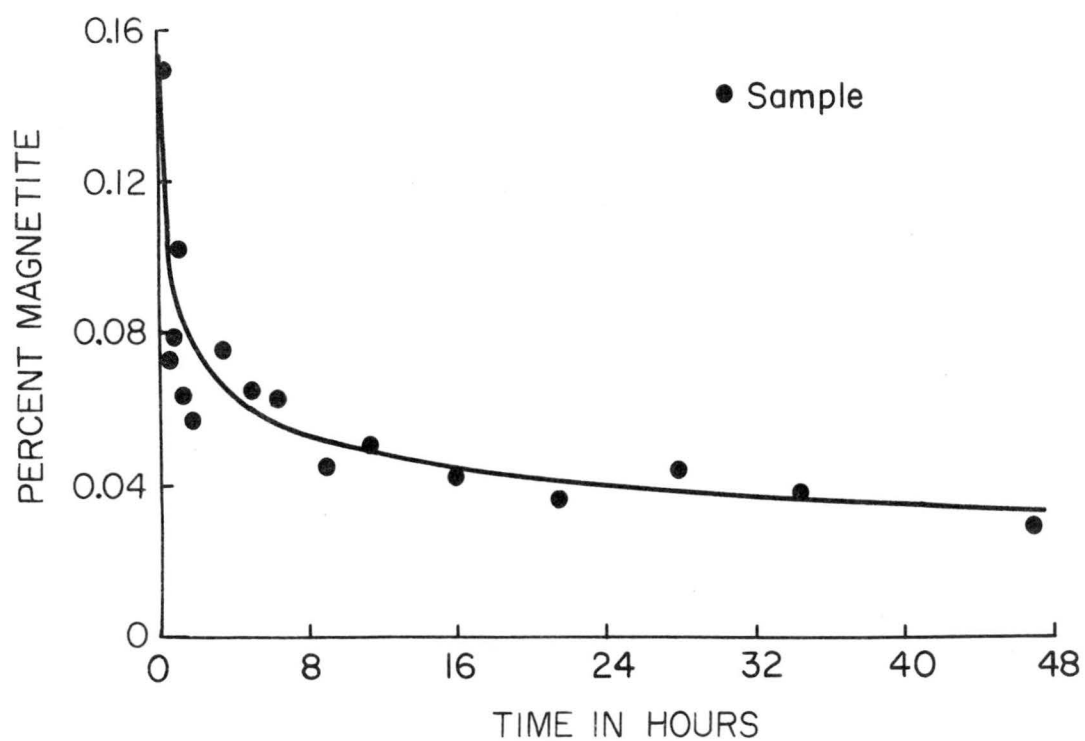
Figure 23.   Relation of magnetite in transport to
             time in 20-cm flume - flat-bed
             conditions.

DISCUSSION OF DATA

Relations among Sediment Samples

Analysis of variance tests of median sizes and shape factors of opaque heavy mineral grains obtained from laminae having high concentrations of opaque heavy minerals show that no significant variance at the 5 percent level existed among sediment samples taken from each of runs 2, 3, and 4. There was, however, a significant difference at the 1 percent level in sorting among the three runs. Among the light minerals from runs 2, 3, and 4 sampled from laminae adjacent to the opaque mineral laminae, a significant difference existed in the median size at the 5 percent level, and no significant difference (5 percent level) existed for the sorting values.

Sorting values determined for opaque heavy mineral samples from run 4 were much larger than for those from other runs. Sorting values for opaque heavy mineral samples of run 4 were close to those of dark opaque grains in the bed material samples. This indicates that all sizes of the high density material in run 4 were being moved by the flow, while sorting of opaque heavy minerals towards finer sizes was occurring in runs 2 and 3.

Sorting is the grain distribution parameter most affected by the different hydraulic conditions. In the flat-bed flow (run 4) segregation apparently occurred at the base of the bed load, and formed a widespread layer of opaque heavy mineral grains. As local erosion of the bed occurred, the opaque minerals became concentrated at the base of the flow and subsequent deposition allowed preservation of the dark laminae. For such a concentrating mechanism, the sorting would have a wide range of values and would depend on the ability of the local flow to sort the sample as to size. In the dune flows smaller sorting values were obtained. This shows that sorting as to size is accomplished more efficiently in the lower flow regime.

Analysis of the critical shear conditions for grain movement indicates that the larger low density grains of the bed material require a much smaller shear for movement than the smaller, more dense grains. Relations of velocities of heavy minerals and light density minerals (figure 3, 4) and the critical shear relationship of opaque heavy minerals to the bed material sample (figure 1, 22) all seem to support the idea that the less dense grains are much more readily entrained and moved. In addition, the difference in size between the low density grains and the high density grains leads to a "hiding effect" that can effectively shield the smaller grains from the flow.

A large percentage of the light mineral grains and opaque heavy mineral grains in adjacent laminae had fall velocities in the same range. However, comparison of fall velocities of median sizes of the dark opaque mineral samples and light mineral samples from the core samples showed that no correlation exists (correlation coefficient of .369) for the median values of these two groups. The light mineral samples were obtained from within (5 samples) and adjacent to (18 samples) the opaque heavy mineral laminae. All the light mineral samples examined were taken from positions within 2 mm of the sampled heavy mineral laminae. The lack of correlation, and the presence of distinct segregated laminae, even though an adequate supply of both mineral groups having equal fall velocities was available, suggest that factors other than grain fall velocity were important to the occurrence of local sorting.

Gross transfer of the sediment load, however, may be related to the fall velocities. This relation is suggested by the bed-material samples in which the fall velocities of 78 percent of the opaque heavy mineral grains overlap those of 74 percent of the light mineral grains in the size distribution range between the 16th and 84th percentiles.

Turbulence is more intense in the trough region than on the higher portions of the stoss side or near the brink point of the dune; and, in general, turbulence is more intense near the bed. A large shear stress at the bed, caused by the turbulent eddies, is probably an important factor in the movement of the opaque heavy minerals, especially in the region of the reattachment point.

Intermittency of turbulence was not studied quantitatively, but strong turbulent eddies passing over the crestal region were observed in the flow and the presence of the strong intermittent turbulence is suggested by the laminae of opaque heavy minerals in the topset beds. Strong turbulence which increases the local shear could cause a rapid movement of the opaque heavy mineral grains from the crest line toward the brink line--and the low density material could then move rapidly over the dense grains or be carried temporarily in suspension. With a decrease in turbulence, the heavy minerals would be deposited before the light minerals.

Bed Forms and Hydraulic Variables

Observations of the four runs in this study and other experimental
runs made in the large flume, as well as field observations, indicate
that the bed configuration is the most important single factor affecting
the opaque heavy mineral segregation. Bed configuration, however, is not
an independent variable but is dependent on a large number of hydraulic
variables as shown by Simons and Richardson (1966, p. 13-16). Among
the most important variables affecting the bed forms are the energy
slope, depth of flow, physical properties of the bed material, and
velocity of flow. In flume studies, flow velocity is considered to be
dependent on the energy slope and depth of flow; however, in field
relations velocity is the independent variable and depth of flow is
probably the dependent variable.

Under the flow conditions of this study there appears to have been three fundamental types of heavy mineral segregation.

1. Thin accumulations of opaque heavy minerals covering small areas, associated with dunes without topset beds and the stoss slope of large dunes with topset beds.

2. Accumulations of opaque heavy minerals associated with topset deposits of large dunes.

3. Accumulations of opaque heavy minerals that were associated with flat-bed movement of the sediment.

The small areas of thin accumulations of opaque heavy minerals were found in association with ripples and small dunes. On larger dunes small areas of heavy mineral accumulations formed on the dune stoss slope, commonly in the areas just downstream from the reattachment point of the flow (the location where the flow impedes on the bed after it passes over the upstream dune front). The accumulations of opaque heavy minerals moved up the stoss side of the dune as units and additional grains were added to the migrating areas during their movement. As erosion and transportation of the sediment occurred all along the stoss slope of the dune, the downstream movement of the opaque heavy mineral grains in these thin accumulations is best explained by their greater resistance to movement resulting in a much slower movement than that of the light mineral grains. The opaque heavy mineral accumulations appeared to move slowly up the dune while the light minerals move rapidly past the heavy mineral area. Dark opaque heavy mineral accumulations generally moved as very thin ripples having very large length to height ratios (figure 10B).

The buildup and movement of these accumulations may be described somewhat as follows. The intense turbulence associated with the reattachment point supplies both heavy and light material to the section just downstream of the reattachment point. Before segregation occurs the bed at this section consists primarily of rather coarse foreset material. This coarse bed material serves as an effective trap for the small dense particles supplied to the area (figure 1, 22). As more and more of the dense particles are trapped and segregated at this location a small area of the bed will become covered by the dense particles. Once the bed has become covered at one location this area becomes more resistant to erosion (figure 22) and the erosion of the light particles around the heavy mineral area tends to expose the accumulation to increasingly stronger flow conditions. Finally the segregated accumulation starts to move up the stoss slope of the dune as the dense particles are eroded from the upstream edge of the accumulation, move across the relatively smooth surface of the heavy mineral area and are deposited at the downstream edge of accumulation. All during this process large quantities of the larger less dense particles are transported over the smooth surface of the accumulation.

Large areas of opaque heavy mineral accumulations often were associated with topset deposits that occurred on large dunes and transition bed forms. The greatest thicknesses of accumulations of dark opaque mineral grains were associated with this type of deposit. Three different situations associated with the topset accumulations of opaque heavy mineral grains were: (1) Accumulations that occurred along the crestal region of the dunes. These opaque heavy mineral accumulations moved downstream with the dune if the dune maintained approximately the same shape and height. Losses from the crestal region were offset by additions of heavy minerals from upstream areas. (2) Laminae of opaque heavy minerals that occurred downstream of the crest line were found both upon and within the topset beds. These heavy mineral deposits were derived from a crestal accumulation. (3) Foreset laminae of opaque heavy mineral grains. The segregated opaque heavy mineral laminae in the foreset could be traced up slope in many cases into the topset beds. The foreset accumulations were caused by conditions similar to those that deposited the opaque heavy mineral laminae in the topset beds except that the heavy mineral grains were transported in sufficient quantities past the brink point to allow some to slide down the lee slope and form the concentrated laminae in the foreset beds. Degree of concentration of opaque heavy mineral grains within laminae decreased with distance down the foreset, indicating a diluting of the opaque heavy minerals with low density grains or a decrease in the proportions of opaque heavy minerals transported to that point.

When accumulations of opaque heavy minerals are deposited just past the brink line in the foreset beds, a periodicity of transport is indicated by the alternation of light with heavy mineral layers in the foreset sequence (figure 14A). This pattern can best be explained by intermittent conditions of strong turbulence. The intermittent turbulent eddies cause increased motion of the high density grains that can result in moving them past the brink point. Most of the lower density material is either carried into suspension by the increased turbulence or moved rapidly over the small, high density grains.

The bed surface elevation of flat-bed flow under equilibrium conditions varied randomly with time but by only a few centimeters from a mean elevation at any location. Therefore, for thick laminae of opaque heavy minerals to form in a flat-bed flow it is important that a flow condition that produces a deep scour (in this study, a transition flow) occur prior to the flat-bed flow. This is necessary in order to segregate the heavy minerals from a thick section of bed material and expose them to the flat-bed flow.

During the flat-bed run, accumulations of opaque heavy minerals occurred near the base of the tractive load. Other accumulations of opaque heavy minerals that were present within the flat-beds probably represent deposits of heavy minerals deposited in a manner similar to the way the opaque heavy mineral beds at the base of the flat beds were deposited but subsequent to deposition of the lower accumulations. Results of the 20 cm flume experiment show a decrease with time in the volume of heavy mineral grains transported in a flat-bed flow at near equilibrium conditions. This decrease in heavy mineral transport indicates that a large percentage of the heavy minerals were deposited early during the flow and the heavy minerals either remained at rest or were reentrained at a rate that was less than the rate of deposition.

On dunes, the thickest accumulations of opaque heavy minerals occurred in the topset bed area near the crest of the dune. Runs 2 and 3 had large dunes with topset beds with a fairly large crest-to-brink distance and large areas of thick accumulation associated with them, while dunes of run 1 had a crest line corresponding to the brink line, with no topset beds and no large areas of concentrated heavy minerals.

In order to determine why the opaque heavy minerals form the large accumulations near the crest of dunes, consider the expression for the rate of sediment transport as given by Simons, Richardson, and Nordin (1965b)

$$\frac{\partial y}{\partial t} + \frac{1}{1-\lambda} \frac{\partial q_b}{\partial x} = 0 \tag{22}$$

where y = elevation of the bed surface, t = time, λ = porosity of the sand bed, q_b = bed load transport rate in volume per unit time per unit width, and x = distance along the bed surface in the direction of the flow. This equation states that the rate of change of bed elevation with time (i.e. the rate of deposition or erosion) is proportional to the rate of change of bed load transport with respect to distance. Applying this equation upstream of the crest of a dune, it is apparent that this is a region of erosion. Erosion is needed in order to keep the thin accumulations on the stoss slope of the dunes exposed to the flow so that they continue to move. However, downstream of the crest of the dune $\partial y/\partial t$ is positive indicating that this is a region of general deposition. Because of their large resistance to motion, dark opaque minerals are selectively deposited from the moving bed load after it passes over the crest. The net result is that the thin accumulations move up the stoss slope of the dune and are deposited just downstream of the crest. At this point the heavy·minerals accumulate to rather large thicknesses because the material is transported out of the region only by occasional bursts of extreme turbulence. Thick accumulations probably could not build up in run 1 because the crest and brink line were coincident and the brink point is a place where the grains can be lost to suspension and to the foreset material.

Topset beds were deposited with a small dip angle in the downstream direction (generally 4° to 6°) between the crest line and the brink line. In general appearance the topset beds resembled planar beds of a flat-bed run.

The topset beds are generally composed of material which is finer than the bed material generally. At first, this appears as a curious anomaly since, as can be seen from equation 22, the crestal region represents the region of the flow where the transport capacity of the flow is greatest. The topset material must be selectively deposited from the moving load that passes the crest. The particles with the greatest resistance to motion should be deposited first. Thus, the segregation by the flow, i.e. deposit of the finer material in the top-set beds and transport of the coarse material on to the brink point, indicates that the trend of the resistance to motion with increasing sieve size is opposite to that indicated in figure 22. This reverse trend has been predicted by qualitatively adjusting figure 22 using the information provided in figure 1 and by the results of the experiment presented in table 4. Results of field experiments by Rathbun, Kennedy, and Culbertson (1971, p. 143-145) show that up to a limiting size, the coarser material in a flat-bed flow has greater velocities than the central sizes of the grain distribution.

CONCLUSIONS

1. The type of bed configuration appears to be the most important factor affecting local segregation of heavy minerals in an open channel flow. Bed configuration, however, is not an independent variable but is dependent on a large number of hydraulic variables, the most important being energy slope, depth of flow, velocity of flow, and the physical properties of the bed material.

2. Three fundamental types of heavy mineral accumulations were observed in this study.

   a. Small areas of thin accumulations of opaque heavy minerals that were associated with the stoss side of dunes. They move as thin ripples and commonly originate in the area just downstream of the reattachment point.

   b. Accumulations of opaque heavy mineral grains that were associated with the topset deposits of large dunes. These accumulations often formed thick deposits along and adjacent to the crestal area of the dune. Opaque heavy mineral segregations were also present within the topset beds, at the surface between the crest line and brink line, and in some cases formed deposits in the foreset beds. The segregated layers in the foreset beds were probably due to mass transport of heavy minerals from the topset area past the brink line by strong conditions of turbulence.

c. Accumulations of opaque heavy minerals that were associated with the flat-bed flows. The thickest and most widespread of the flat-bed segregations of heavy minerals generally occurred at the base of the flat beds, but additional laminations of heavy minerals were present in the flat beds formed by the flow.

3. Among the sediment properties of size, sorting, and shape obtained for opaque heavy minerals from core samples taken from the bed, the only significant variance that occurred between runs 2, 3, and 4 was a difference in the sorting of the opaque heavy mineral grains.

4. Theoretical considerations indicate a distinct difference exists in the transport rates of spheres of different densities moving as bed load. The initiation of motion of grains is illustrated by the Shields diagram (figure 5). Based on the Shields criteria, curves can be developed that show the relationship between critical shear and grain size for materials of different densities. Curves were constructed and they clearly show that the opaque heavy minerals are much more resistant to motion than the light minerals.

5. Theoretical analysis and experimental results illustrate that the size of the particle in transport as well as the size of the bed material affects the resistance of a particle to tractive motion. For the particle sizes of interest in this study, it is found that a particle's resistance to tractive motion over a poorly sorted bed material decreases with increasing particle size at least in the size range studied.

6. Fall velocity values for median sizes of opaque heavy mineral grains and associated light minerals from laminae adjacent to or within the opaque mineral laminae are not correlated. This lack of correlation and the presence of distinct segregated laminae, suggests that fall velocity alone has little or no effect on the local sorting of heavy minerals.

REFERENCES

Allen, J. R. L., 1968, Current ripples--their relation to patterns of
water and sediment motion: North-Holland Publishing Co., Amsterdam,
433 p.

American Society of Civil Engineers, Task Committee on Preparation of
Sedimentation Manual, 1962, Introduction and properties of sediment:
Am. Soc. Civil Engineers, Proc., v. 88, no. HY4, p. 77-107.

_____, 1966, Sedimentation transportation mechanics: Initiation
of motion: Am. Soc. Civil Engineers Jour., v. 92, no. HY2, p. 291-314.

_____, Task Force on Bed Forms in Alluvial Channels, 1966,
Nomenclature for bed forms in alluvial channels: Am. Soc. Civil
Engineers, Proc., v. 92, no. HY3, p. 51-64.

Bagnold, R. A., 1966, An approach to the transport problem from general
physics: U. S. Geol. Survey Prof. Paper 422-I, 37 p.

Brady, L. L., 1971, An experimental study in a large flume of heavy
mineral segregation under alluvial flow conditions: Ph.D.
dissertation, The University of Kansas, Lawrence, Kansas, 115 p.

Coleman, N. L., 1967, A theoretical and experimental study of drag and
lift forces acting on a sphere resting on a hypothetical streambed:
Internat. Assoc. Hydraulic Research Cong., 12th, Proc., Fort Collins,
Colorado, U.S.A., v. 3, p. 185-192.

Corey, A. T., 1949, Influence of shape on the fall velocity of sand grains:
M. S. thesis, Colorado State University, Fort Collins, Colorado,
102 p.

Daily, J. W. and Harleman, D. R. F., 1966, Fluid dynamics, Addison-Wesley
    Publishing Co., Reading, Mass. 454 p.

Einstein, H. A., 1950, The bed load function for sediment transportation
    in open channel flows: U. S. Dept. Agriculture Tech. Bull. 1026,
    70 p.

_____, and Chien, N., 1953, Transport of sediment mixtures with
    large ranges of grain sizes: University of California Institute of
    Engineering Research, Berkeley, California, 49 p.

El-Sammi, E. A., 1949, Hydrodynamic forces on particles in the surface of
    a stream bed: Ph.D. dissertation, The University of California at
    Berkeley, Berkeley, California.

Grigg, N. S., and Rathbun, R. E., 1969, Hydraulic equivalence of minerals
    with consideration of the reentrainment process in Geological Survey
    Research 1969: U. S. Geol. Survey Prof. Paper 650-B, p. 77-80.

Guy, H. P., Simons, D. B., and Richardson, E. V., 1966, Summary of
    alluvial channel data from flume experiments: U. S. Geol. Survey
    Prof. Paper 462-I, 96 p.

Henderson, F. M., 1966, Open channel flow: The MacMillan Co., New York,
    522 p.

Ippen, A. T., and Verma, R. P., 1955, Motion of particles on bed of
    a turbulent stream: Am. Soc. Civil Engineers Trans., v. 120, p.
    921-939.

Kennedy, J. F., 1963, The mechanics of dunes and antidunes in erodible-
    bed channels: Fluid Mechanics Jour., v. 16, p. 521-544.

Lane, E. W., 1947, Report of the Subcommittee on Sediment Terminology: American Geophysical Union Trans., v. 28, p. 936-938.

McQuivey, R. S., and Keefer, T. N., 1969, The relation of magnetite over ripples in Geological Survey Research 1969: U. S. Geol. Survey Prof. Paper 650-D, p. 244-247.

Rathbun, R. E., Kennedy, V. C., and Culbertson, J. K., 1971, Transport and dispersion of fluorescent tracer particles for the flat-bed condition, Rio Grande Conveyance Channel, near Bernardo, New Mexico: U. S. Geol. Survey Prof. Paper 562-I, 56 p.

Raudkivi, A. J., 1967, Loose boundary hydraulics: Pergamon Press, Oxford, 331 p.

Richardson, E. V., and McQuivey, R. S., 1968, Measurement of turbulence in water: Am. Soc. Civil Engineers Proc., v. 94, no. HY2, p. 411-430.

Rittenhouse, G., 1943, Transportation and deposition of heavy minerals: Geol. Soc. American Bull., v. 54, p. 1725-1780.

Rubey, W. W., 1933, The size distribution of heavy minerals within a waterlaid sandstone: Jour. Sed. Petrology, v. 3, p. 3-29.

Schultz, E. F., Wilde, R. H., and Albertson, M. L., 1954, Influence of shape on the fall velocity of sedimentary particles: U. S. Army Corps of Engineers, Missouri River Div., MRD Sediment Ser., no. 5, 161 p.

Sears, F. W., and Zemansky, M. W., 1963, University physics, 3rd ed., pt. 1: Addison-Wesley Publishing Co., Reading, Mass., 548 p.

Sheen, S. J., 1964, Turbulence over a sand ripple: M. S. thesis, University of Auckland, New Zealand.

Shields, A., 1936, Anwendung der Ahnlichkeitsmechanik und der
    Turbulenzforschung auf die Geschiebebewegung: Mitteilungen der
    Press. Versuch anst. f. Wasserbau u. Schiffbau., Berlin, no. 26,
    26 p.; Application of similarity principles and turbulence research
    to bed load movement--translated to English by W. P. Ott and J. C.
    van Uchelen, U. S. Dept. Agriculture, Soil Conservation Service
    Coop Lab., Calif. Inst. Tech., Pasadena, 21 p.

Simons, D. B., and Richardson, E. V., 1963, Forms of bed roughness in
    alluvial channels: Am. Soc. Civil Engineers, Trans., v. 128, p.
    284-302.

_____, 1966, Resistance to flow in alluvial channels: U. S.
    Geol. Survey Prof. Paper 422-J, 61 p.

Simons, D. B., Richardson, E. V. and Nordin, C. F., Jr., 1965a, Forms
    generated by flow in alluvial channels: Soc. Econ. Paleontologists
    and Mineralogists Spec. Pub. 12, p. 34-52.

_____, 1965b, Bed load equations for ripples and dunes: U. S.
    Geol. Survey Prof. Paper 462-H, 9 p.

Sokal, R. R., and Rohlf, F. J., 1969, Biometry: W. H. Freeman and Co.,
    San Francisco, 776 p.

Streeter, V. L., 1966, Fluid Mechanics, 4th ed.: McGraw-Hill Book Co.,
    New York, 705 p.

Tourtelot, H. A., 1968, Hydraulic equivalence of grains of quartz and
    heavier minerals, and implications for the study of placers: U. S.
    Geol. Survey Prof. Paper 594-F, 13 p.

U. S. Inter-Agency Committee on Water Resources, 1957, Some fundamentals of particle size analysis, in A study of methods used in measurement and analysis of sediment loads in streams: Washington, U. S. Govt. Printing Office, Rept. 12, 55 p.

_____, 1958, Operator's manual on the visual-accumulation-tube method for sedimentation analysis of sands, Report K: St. Anthony Falls Hydraulic Laboratory, Minneapolis, Minn., 30 p.

Watters, G. Z., and Rao, M. V. P., 1971, Hydrodynamic effects of seepage on bed particles: Am. Soc. Civil Engineers Proc., v. 97, no. HY3, p. 421-439.

APPENDIX

A. Symbols and Nomenclature

B. Grain-Mount Preparation and Relationship of Direct Grain
    Measurements to Sieve-Size Equivalents

C. Analyses of Opaque Heavy Mineral Grains and Light Mineral
    Grains from Core Samples (Runs 2, 3, 4)

D. Sediment Concentration and Size Analyses of Suspended
    Sediment Samples

APPENDIX A

Symbols and Nomenclature

Symbol	Definition
A	area, such as the cross sectional area of the flume
A_s	projected area of a sphere
a	longest diameter of a grain for three mutually perpendicular axes
b	intermediate diameter of a grain for three mutually perpendicular axes
C_D	coefficient of drag for a sediment particle. The coefficient of drag varies with the particle geometry, relation of particle shape to flow, and the Reynolds number of the flow
C_F	coefficient of friction for a sediment particle. The coefficient of friction depends primarily on the nature of the particle surface and the surface of the material with which it is in contact
C_L	coefficient of lift for a sediment particle. The coefficient of lift depends on the shape of the particle, relation of particle shape to flow, and the Reynolds number of the flow
C_R	coefficient of static resistance of a sediment particle. The coefficient of static resistance depends on the shape and size of the particle and the arrangement, size, and shape of the bed particles
c	shortest diameter of a grain with three mutually perpendicular axes
D	flow depth
d	diameter of a spherical particle
d_B	diameter of spheres making up a bed material
d_m	diameter of a sphere resting on the bed
d_s	diameter of a grain--equal to sieve diameter or approximately equal to b-diameter of a particle
F_D	hydrodynamic drag force--force exerted by the flow on the particle parallel to the relative motion of the flow

116

Symbol	Definition
F_F	frictional force--resistance to motion between two bodies in contact
F_G	gravity force
F_L	hydrodynamic lift force--the force component produced by the flow on a particle that is perpendicular to the direction of the flow and opposing the gravity force
F_N	resultant force normal to the bed surface
F	Froude number = $\overline{U}/\sqrt{gD}$ --A ratio of inertial forces to gravitational forces
g	gravitational constant (980 cm/sec^2)
H	dune height--vertical distance from trough point to crest point
k	ratio d_m to d_B
L	dune length--measured from trough of a given dune to trough point of the next dune upstream
n	number count of a given size in grain size analysis
Q	fluid discharge (cubic meters/sec)
q_B	bed-load discharge--weight of sediment carried in bed load per unit width/unit of time
q_b	bed-load discharge--volume per unit width/unit time
Re	Reynolds number $= \dfrac{\overline{UD}}{\nu}$ --a ratio of inertial forces to viscous forces for the mean flow
R_*	particle Reynolds number = U_*d/ν --a ratio of inertial to viscous forces relative to a particle
R'	hydraulic radius a channel would have if the resistance to flow was limited to grain roughness (no resistance due to bed form or stream bank roughness). This term can be stated in terms of the average flow depth (D) with corrections for bed form roughness
S	energy slope of the fluid
t	time

Symbol	Definition
U	fluid velocity
$\bar{U}$	mean fluid velocity
U_*	shear velocity $= \sqrt{\tau_o/\rho}$. The shear velocity is not a real velocity but is related to the real velocity which would give rise to shear stress τ_o (Henderson, 1966, p. 412).
V_f	velocity of flow at a representative distance from the bed
V_o	relative velocity of flow past a body
V_s	velocity of translation of a particle
W	channel width
x	distance along bed surface
Y	height above the bed surface
y	elevation of the bed surface
γ	specific weight of water
γ_s	specific weight of a sediment grain
η	eddy viscosity that depends on the state of turbulent motion
θ	angle between the bed and horizontal line
λ	porosity of the bed
μ	dynamic viscosity of the fluid
ν	kinematic viscosity of the fluid $= \dfrac{\mu}{\rho}$ --a ratio of viscosity to mass density
ρ	mass density of water
ρ_s	mass density of a particle

Symbol	Definition

σ geometric standard deviation of a sediment size distribution

$$\sigma = \frac{1}{2}\left(\frac{d_{50}}{d_{16}} + \frac{d_{84}}{d_{50}}\right)$$

τ shear stress in the fluid. For turbulent flow $\tau = (\mu+\eta)\frac{dU}{dY}$ and for laminar flow

$$\tau = \mu\frac{dU}{dY}$$

τ_o average shear stress at the bed = γDS--force per unit area acting on the bed in the direction of flow

τ_c critical shear stress for sediment particles--the minimum amount of shear stress necessary to start movement of particles at the bed

τ_* dimensionless shear stress (Shields entrainment function) =

$$\frac{\tau_c}{(\gamma_s-\gamma)d_s}$$

Φ Einstein's intensity of bed-load transport

ψ Einstein's intensity of shear on a particle

119

APPENDIX B

Grain-Mount Preparation and Relationship of Direct Grain Measurements to Sieve-Size Equivalents

Preparation of Grain Mounts--Grain mounts for size analyses were prepared for the bed material sample, core samples and many of the suspended sediment samples studied. Where loose sample grains were used, such as the bed material sample, the sample was reduced by a microsplitter to the desired size. For samples of opaque heavy mineral grains and light mineral grains that were obtained from select laminations or area of a grouted core, the material was removed by use of a blunted dissecting needle. Both types of samples were prepared by distributing the grains as evenly as possible onto a petrographic slide that had previously been covered with alcohol. The grains, in settling through the alcohol, oriented themselves with their shortest axis (c-axis) perpendicular to the slide. Measurement of 500 grains for shape factor analysis showed that this orientation occurred for 88 percent of the grains. Those grains with the c-axis lying parallel to the slide usually had a c-axis length very similar to the intermediate axis (b-axis) length.

When the alcohol evaporated, a residue remained that caused the grain to adhere to the slide. After grain shape studies were made, Lakeside 70 and a cover glass were applied for permanent mounting and grain size measurement.

Sieve-Analysis Equivalent of Direct Measurement--Mounted mineral
grains were measured directly by use of a petrographic microscope with
a calibrated eyepiece that was divided into units of 12.1 microns.
For most samples, intermediate axes (b-axis) were measured in unit
sizes on 200 grains per slide. Where more than 200 measurements were
used for a given sample, additional slides were made.

If an abundance of material was available, such as the bed-material
sample, grains were selected by an equal-interval point-count method. A
pattern of evenly spaced intervals was made by use of a modified stage
micrometer mounted on the microscope. If a grain was present under the
stage stop, that grain was measured. A stage interval was selected
that was large enough to prevent repetition of individual grain
measurements.

Slides made from samples with limited amounts of material (samples
from grouted cores) were analyzed by a line measurement technique. In
the line method, horizontal traverses were made over the slide at equal
intervals and the b-axis was measured for each grain of the particular
mineral being studied that the line crossed.

The probability of a grain being measured by the point method is
in direct proportion to its projected area on the slide, while
the probability of a grain being "hit" by the line method is in direct
proportion to the diameter of a grain perpendicular to the traverse line.
Neither of these methods, however, allows for differences in the thick-
ness of the grains perpendicular to the slide.

Opaque heavy minerals and light minerals were studied separately, and both groups had mean shape factors (Appendix C) of near equant shape (0.68 to 0.75 shape factor); therefore, a relation between measured size and weighted sieve equivalence was determined.

In order to make the direct measurements equivalent to the weight-size equivalents determined by sieving, a common measuring factor was used. The best common standard for such a relation was the nominal grain diameter defined as the diameter of a sphere that has the same volume as the particle (Lane, 1947, p. 937). The U. S. Inter-Agency Committee on Water Resources (1957, p. 31, 33-35) developed graphs from extensive studies that show the relation of the intermediate axes of grains to their nominal diameters and the sieve size equivalents of grains to their nominal diameters for various shape factors. Based on the graphs of the U. S. Inter-Agency Committee on Water Resources (1957, figure 4, 5), the sieve diameter equivalent of the grains is 0.85 times the value of the direct intermediate axis measurement (using a shape factor of 0.7) for the grain sizes in this study.

Besides differences in b-axis and sieve-size measurement, other factors had to be considered for conversion of direct measurement to weight frequencies of a sieve analysis including differences in grain thickness for different grain sizes as well as the probability that a certain size grain occurred in the measurement in its correct proportion relative to the total grain-size population. Differences in grain thicknesses were corrected by multiplying the b-size frequency count by the b-axis diameter. To compute a weight frequency distribution from direct measurement, the following manipulations of the direct b-axis measurements were made.

1. For the line method, the size frequency was determined by taking the percentage of each size from the sum of the sizes determined by Σnb^2 where n is the b-axis frequency, b is the b-axis size.

2. For the point-count method, the size frequency was determined by taking the percentage of each size from the sum of the sizes determined by Σnb.

Cumulative curves were plotted with the weight percentages as the ordinate and with the b-axis values multiplied by 0.85, the correction factor, on the abscissa.

A check of the 0.85 conversion factor was made by using the bed-material sample. The results showed close agreement to a sieve analysis of the same material except on the large grain size end (figure 9). Direct measurement of the b-axis of 1,000 grains showed a weighted median value of 0.338 mm and a sorting (σ) of 1.56. A sieved sample of the same bed material gave a median value of 0.285 mm and a sorting of 1.58. Sorting of the sieve and weighted direct measurements were similar. Applying the correction factor of 0.85 to the median diameter of 0.338 mm determined by direct measurement gives a corrected value of 0.289 mm, which is in good agreement with the median diameter of 0.285 mm determined from sieve data.

Values stated in the text of this study for a given grain-size measurement are the sieve-size equivalent values determined by the above described method and by using 0.85 as the size conversion factor.

APPENDIX C

Analyses of Opaque Heavy Mineral Grains and Light Mineral Grains
from Core Samples (Runs 2, 3, 4)

Data on size and sorting shown for each of the samples in

tables 5 and 6 were determined from direct measurement of 200

Tables 5 and 6 (p. 126, 127, 128, 129, 130, 131, 132, 133) near here

---

individual grains using techniques described in Appendix B. The bed-

material size analyses, however, were based on 1,000 measurements.

Twenty grain measurements per sample were made for determination

of mean shape factor. The shape factor used in this report was

originally defined by Corey (1949) as

$$S.F. = \frac{c}{\sqrt{ab}}$$

for three mutually perpendicular axes of the grains, where

a = maximum diameter of the grain

b = intermediate diameter of the grain

c = smallest diameter of the grain

Table 5. Size analyses of opaque heavy minerals from core samples.

Sample	Median d_{50} (mm)	d_{16} (mm)	d_{84} (mm)	Sorting (σ)	Shape Factor	Description of Location in Bed*
Bed Material	.144	.099	.220	1.49	.684	Representative sample of Bed Material
				RUN 2		
B-47-B-1	.140	.098	.180	1.36	.735	Foreset, 2 mm dark mineral streak with interspersed light density minerals (Sta. 86, 1.06 m right of center line)
B-47-X-1	.133	.104	.158	1.23	.747	Topset, 7 mm dark mineral zone near surface (Sta. 176, 1.00 m left of center line)
B-47-36-1	.105	.083	.150	1.34	.715	Topset, dark mineral zone (0.5 mm), 3 mm below the surface (Sta. 100, 0.61 m right of center line)
B-47-37-1	.115	.081	.155	1.39	.711	Topset, dark mineral zone (1 mm), 1.5 mm below the surface (Sta. 96, 0.61 m left of center line)
B-47-46-1	.132	.103	.162	1.25	.711	Brink point, dark mineral zone (1 mm), 4.5 mm below the surface (Sta. 85, 0.61 m left of center line)
B-47-46-2	.140	.107	.176	1.28	.718	Foreset, downstream from B-47-46-1, same dark mineral streak but with light density minerals interspersed (Sta. 85, 0.61 m left of center line)
B-47-47-1	.112	.087	.138	1.26	.698	Topset, dark mineral zone (3 mm), 5 mm below the surface (Sta. 85, on center line)
RUN 2 Ave.	.125	.095	.160	1.30	.719	

Table 5. (continued)

Sample	Median d_{50} (mm)	d_{16} (mm)	d_{84} (mm)	Sorting (σ)	Shape Factor	Description of Location in Bed*
				RUN 3		
B-48-A-1	.126	.101	.154	1.23	.754	Topset, thickest laminae in zone, 1.5 mm thick of several thin dark mineral laminations; 5 mm from surface (Sta. 98, 1.07 m right of center line)
B-48-B-1	.154	.102	.198	1.40	.744	Topset (near Brink point), dark mineral zone (1 mm) at base of topset 3 mm from surface (Sta. 114, 0.79 m left of center line)
B-48-B-2	.150	.115	.192	1.29	.769	Foreset, 2 mm dark mineral zone with interspersed light density minerals (Sta. 114.2, 0.79 m left of center line)
B-48-10-1	.087	.063	.111	1.33	.724	Flat Bed, dark mineral zone (0.5 mm) 35 mm from the surface (Sta. 18, 0.61 m left of center line)
B-48-37-1	.124	.099	.161	1.28	.721	Topset, thick dark mineral zone (4 mm) at the surface (Sta. 94, 0.61 m left of center line)
B-48-40-1	.122	.088	.154	1.32	.723	Topset, uppermost dark mineral laminae (0.5 mm) in dark mineral zone 17 mm from surface (Sta. 90, 0.61 m left of center line)
B-48-52-1	.110	.082	.145	1.33	.751	Topset, dark mineral zone (0.5-1 mm) 4 mm below the surface (Sta. 74, 0.61 m left of center line)
RUN 3 Ave.	.125	.093	.159	1.31	.741	

127

Table 5. (continued)

Sample	Median d$_{50}$ (mm)	d$_{16}$ (mm)	d$_{84}$ (mm)	Sorting (σ)	Shape Factor	Description of Location in Bed*
			RUN 4			
B-46-5-1	.144	.102	.218	1.46	.744	Dark mineral zone (1.5 mm) at base of flat-bed sands, 6 mm from surface (Sta. 176, on center line)
B-46-12-1	.100	.076	.120	1.26	.715	Dark mineral zone (1 mm) at base of flat-lying sand, 8 mm from surface (Sta. 168, 0.61 m right of center line)
B-46-20-1	.135	.095	.173	1.35	.693	Dark mineral zone (0.5 mm) interbedded with light density, flat-lying sand, 11 mm from surface (Sta. 110, on center line)
B-46-20-2	.103	.070	.150	1.47	.748	Mixed dark mineral and light density minerals zone (1.5 mm) just below sample B-46-20-1. Taken 20 mm above base of flat-bed sand (Sta. 110, on center line)
B-46-26-1	.147	.095	.201	1.46	.758	Dark mineral zone (1 mm) 6.5 mm from surface, overlain and underlain by light density sand, 22 mm above base of flat-bedded material (Sta. 102, on center line)
B-46-52-1	.150	.082	.205	1.59	.781	Zone of dark minerals with interspersed light density minerals (1 mm), 16 mm below surface, 35 mm above base of flat-bedded sands (Sta. 130, on center line)

Table 5. **(continued)**

Sample	Median d_{50} (mm)	d_{16} (mm)	d_{84} (mm)	Sorting (σ)	Shape Factor	Description of Location in Bed*
			RUN 4 (Continued)			
B-46-55-1	.135	.086	.173	1.43	.757	Dark mineral zone with interbedded light density grains (zone is 2.5 mm thick) at base of flat-bedded material, 15 mm from surface (Sta. 155, on center line)
RUN 4 Ave.	.131	.087	.177	1.43	.742	
Average of three runs	.127	.091	.165	1.35	.735	

*Stations along the flume are designated in feet (1 ft. = 0.3048 m) downstream from the headbox. (Example: the distance between Sta. 100 and Sta. 110 is 10 ft. (3.05 m)).

Table 6. Size analyses of light minerals associated with opaque heavy minerals in the core samples.

Sample	Median d_{50} (mm)	d_{16} (mm)	d_{84} (mm)	Sorting (σ)	Description of Location in Bed*
Bed Material	.287	.190	.462	1.56	Representative sample of bed material
		RUN 2			
B-47-B-2	.201	.150	.247	1.29	Foreset, light mineral zone (2 mm) underlying dark mineral zone sample in B-47-B-1 (Sta. 86, 1.06 m right of center line)
B-47-X-2	.219	.155	.276	1.33	Topset, light mineral zone (1.5 mm) underlying dark mineral zone sampled in B-47-X-1 (Sta. 176, 1.00 m left of center line)
B-47-36-2	.176	.131	.244	1.37	Topset, light mineral zone (2 mm) overlying dark mineral zone sampled in B-47-36-1 (Sta. 100, 0.61 m right of center line)
B-47-36-3	.167	.121	.229	1.38	Topset, light mineral zone (2 mm) underlying the dark mineral zone sampled in B-47-36-1 (Sta. 100, 0.61 m right of center line)
B-47-37-2	.180	.136	.248	1.35	Topset, light mineral zone (1.5 mm) underlying dark zone sampled in B-47-37-1 (Sta. 96, 0.61 m left of center line)
B-47-46-2	.222	.150	.315	1.45	Foreset below brink point, light density grains within the dark mineral zone sampled in B-47-46-2 (Sta. 85, 0.61 m left of center line)
B-47-46-3	.236	.168	.349	1.44	Brink point, light mineral zone (2 mm) overlying the dark mineral zone sampled in B-47-46-2 (Sta. 85, 0.61 m left of center line)
B-47-47-2	.188	.138	.268	1.39	Topset, light mineral zone (2 mm) overlying dark mineral zone sampled in B-47-47-1 (Sta. 85, on center line)

Table 6. (Continued)

Sample	Median d_{50} (mm)	d_{16} (mm)	d_{84} (mm)	Sorting (σ)	Description of Location in Bed*
		RUN 2 (Continued)			
B-47-47-3	.207	.150	.266	1.33	Topset, (low angle), light mineral zone (2 mm) underlying dark mineral zone sampled in B-47-47-1 (Sta. 85, on center line)
RUN 2 Ave.	.200	.144	.271	1.37	
		RUN 3			
B-48-A-2	.236	.170	.309	1.35	Topset, light mineral zone (2 mm) underlying the dark mineral zone sampled in B-48-A-1 (Sta. 98, 1.07 m right of center line)
B-48-B-2	.254	.183	.343	1.37	Foreset, light density minerals from within the zone where dark minerals were sampled in B-48-B-2 (Sta. 114, 0.79 m left of center line)
B-48-B-3	.290	.196	.388	1.41	Foreset, light mineral zone (2 mm) overlying the dark mineral foreset in B-48-B-2 (Sta. 114, 0.79 m left of center line)
B-48-B-4	.212	.151	.280	1.36	Topset (near brink point), light mineral zone (1.5 mm) overlying the dark mineral zone sampled in B-48-B-1 (Sta. 114, 0.79 m left of center line)
B-48-10-2	.243	.173	.305	1.33	Flat Bed, light mineral zone (2 mm) overlying dark mineral zone sampled in B-48-10-1 (Sta. 18, 0.61 m left of center line)
B-48-37-2	.199	.155	.260	1.30	Topset, light mineral zone (2 mm) underlying dark mineral zone sampled in B-48-37-1 (Sta. 94, 0.61 m left of center line)

131

Table 6. (Continued)

Sample	Median d_{50} (mm)	d_{16} (mm)	d_{84} (mm)	Sorting (σ)	Description of Location in Bed*
		RUN 3 (Continued)			
B-48-40-2	.232	.159	.299	1.37	Topset, light mineral zone (2 mm) overlying the dark mineral zone sampled in B-48-40-1 (Sta. 90, 0.61 m left of center line)
B-48-52-2	.200	.141	.332	1.54	Topset, light mineral zone (2 mm) overlying the dark mineral zone sampled in B-48-52-1 (Sta. 74, 0.61 m left of center line)
B-48-52-3	.220	.169	.285	1.30	Topset, light mineral zone (2 mm) underlying the dark mineral zone sampled in B-48-52-1 (Sta. 74, 0.61 m left of center line)
RUN 3 Ave.	.232	.166	.311	1.37	
		RUN 4			
B-46-5-2	.258	.167	.360	1.47	Light mineral zone (2 mm) overlying the dark mineral zone sampled in B-46-5-1 (Sta. 176, on center line)
B-46-12-2	.218	.162	.285	1.33	Light mineral zone (2 mm) overlying the dark mineral zone sampled in B-46-12-1 (Sta. 168, 0.61 m right of center line)
B-46-20-2	.201	.134	.286	1.46	Light density minerals within dark mineral zone sampled in B-46-20-2 (Sta. 110, on center line)
B-46-52-1	.218	.152	.301	1.40	Light minerals directly overlying and within the dark mineral zone sampled in B-46-52-1 (Sta. 130, on center line)

132

Table 6 (Continued)

Sample	Median d_{50} (mm)	d_{16} (mm)	d_{84} (mm)	Sorting (σ)	Description of Location in Bed*
		RUN 4 (Continued)			
B-46-55-1	.227	.136	.362	1.63	Light mineral zone within the zone where dark minerals were
RUN 4 Ave.	.224	.150	.319	1.46	sampled (B-46-55-1). Light minerals separating the very thin dark mineral laminations (Sta. 155, on center line)
Average of three runs	.218	.154	.297	1.40	

*Stations along the flume are expressed in feet (0.3048 m) in a downstream direction.

133

One advantage in the use of the Corey shape factor over other shape factors is the extensive experimental data available on sediment analysis by Schultz, Wilde and Albertson (1954) and a summarization of the work by the U. S. Inter-Agency Committee on Water Resources (1957) where the Corey shape factor was used. Discussion of the Corey shape factor as compared to other shape factors is presented by Tourtelot (1968, p. 4-7)

Measurements of the shape factor as determined for the bed-material sample of opaque heavy minerals and light minerals were each based on 60 shape factor measurements, 20 measurements on each of three grain mount slides.

For example identifying numbers in tables 5 and 6, the following criteria were used: Example   B - 47 - B - 1
                         (1) (2) (3) (4)

(1) The B refers to a "bed" sample as opposed to a "S" for suspended sample (Appendix D).

(2) The 47 refers to a continuous flume experiment series run number. The following numbers are the designated run numbers for this study:

             #45 = Run 1

             #47 = Run 2

             #48 = Run 3

             #46 = Run 4

(3) The <u>B</u> used in the example is a selected core sample. All letters in the third position designate selected samples, while numbers indicate core samples obtained in the established sample network. Numbers and letters used are usually consecutive except for (X) used in run 2.

(4) The <u>1</u> in the fourth position designates the grain mount number made from that particular core sample.

Examples of horizontal core samples obtained from the bed including the cores from which the bed samples of light mineral and opaque heavy mineral grains were obtained are shown in figure 24.

Figure 24 (caption on next page) belongs near here
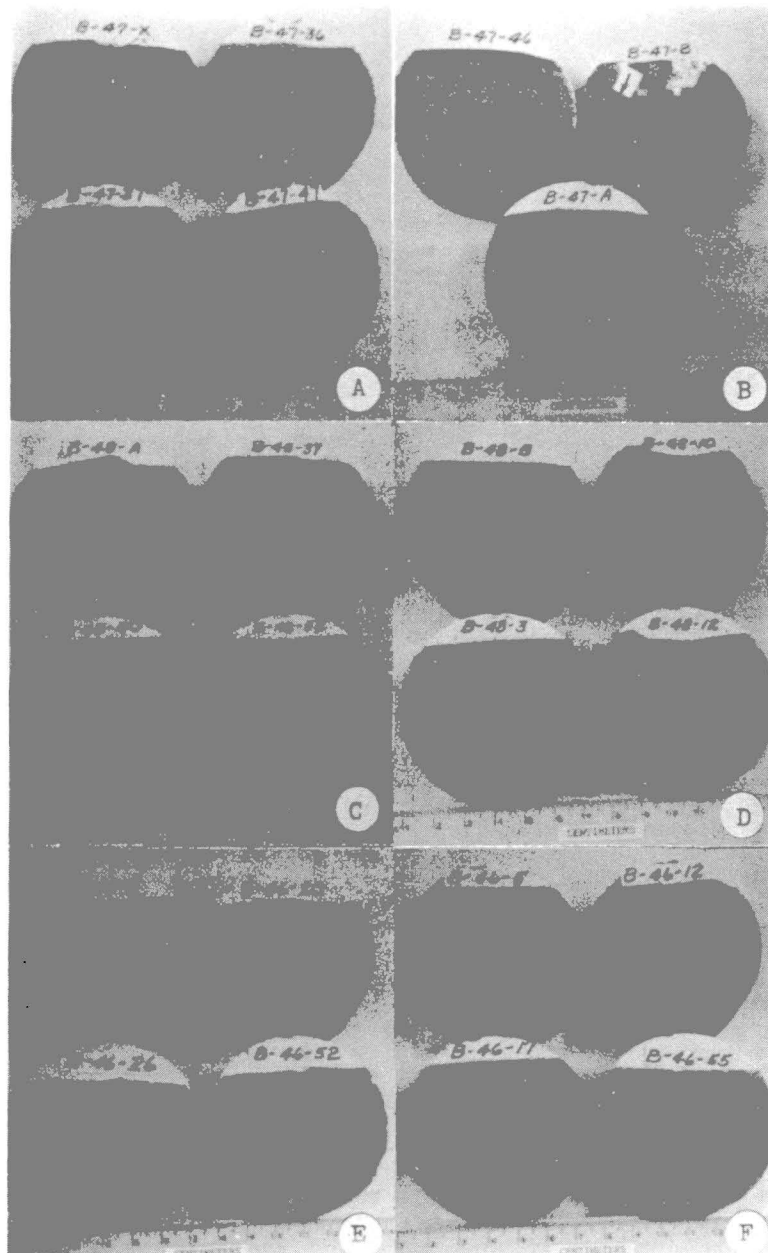

Figure 24. Sections of core samples showing opaque heavy mineral
beds in: (A) Run 2--topset beds (sample B-47-X was
obtained from a crestal accumulation), (B) Run 2--foreset
beds, (C) Run 3--topset beds, (D) Run 3--foreset beds
(sample B-48-B) and flat bed area (samples B-48-3, 10,
and 12), (E) Run 4--within the flat bed deposits, (F) Run
4--at the base of the flat beds.

Sediment Concentration and Size Analyses of Suspended Sediment Samples

Table 7. Size analyses and concentration of suspended sediment samples.

Run	Location	Height above bed (cm)	Conc. (mg/ℓ)	d_{50}	*Size (mm) d_{16}	d_{84}	Sorting (σ)
1	Trough	33.6	122	.146	.116	.184	1.26
		18.3	236	.186	.154	.225	1.21
		9.2	475	.172	.132	.215	1.28
		3.1	501	.172	.134	.217	1.28
	Brink point	24.4	66	.158	.127	.200	1.25
		18.3	130	.143	.108	.179	1.29
		9.2	117	.148	.116	.187	1.27
		3.1	290	.165	.128	.212	1.29
	Stoss side	18.3	291	.174	.140	.207	1.22
		9.2	234	.174	.140	.216	1.24
		3.1	343	.177	.146	.224	1.24
2	Trough	42.7	458	.138	.104	.172	1.29
		30.5	2304	.187	.146	.230	1.26
		24.4	1554	.173	.123	.209	1.31
		9.2	2022	.186	.128	.244	1.38
	Brink point	36.6	176	.127	.092	.157	1.31
		18.3	256	.138	.101	.184	1.35
		12.2	345	.140	.103	.183	1.33
		3.1	551	.145	.110	.184	1.29
	Stoss side	33.6	391	.140	.107	.176	1.28
		21.4	513	.157	.116	.205	1.33
		9.2	569	.146	.107	.190	1.33
		3.1	763	.150	.120	.188	1.25
3	Stoss side	33.6	59	.130	.102	.165	1.27
		18.3	328	.155	.117	.212	1.35
		9.2	279	.144	.112	.184	1.28
		3.1	618	.146	.115	.184	1.26
	Flat bed	27.5	25	.116	.090	.159	1.33
		21.4	39	.119	.096	.150	1.25
		12.2	218	.134	.105	.160	1.24
		7.6	974	.172	.133	.220	1.29
4	Flat bed	33.6	512	.123	.088	.156	1.33
		21.4	940	.136	.099	.168	1.30
		9.2	2103	.151	.110	.195	1.33
		3.1	6477	.183	.133	.226	1.31

*Size determined by VA tube sedimentation analysis